UNIVERSITY OF BIRMINGHAM

MRes Thesis

SCHOOL OF CHEMISTRY

Switchable Biological Surfaces

Minhaj Lashkor

March 2010

SUPERVISORS:

Professor Jon A. Preece

Dr Paula M. Mendes

UNIVERSITYOF
BIRMINGHAM

University of Birmingham Research Archive

e-theses repository

Abstract

The ability to control properties such as wettability and bio-molecule immobilisation onto self-assembled monolayers (SAMs) has many potential biological and medical applications. The aim of this project was to produce mixed biotinylated peptide monolayers that are responsive to an electric potential, thus providing a system in which the conformation of the biotinylated peptides could be switched. This allows for controlled protein immobilisation onto a mixed monolayer. Fluorescence images indicated that less binding took place between the neutravidin and the biotinylated peptide under a negative potential due to decreased image intensity. Control experiments were also carried out using non-biotinylated peptides to show there was minimal non-specific binding and that binding was only taking place on the biotin binding sites.

Stability studies were also carried out using cyclic voltammetry on pure and mixed monolayers to further understand the stability range of the monolayers. High currents were observed in cyclic voltammograms of pure and mixed SAMs. In order to identify the cause of the high current readings, further samples were investigated of well known SAMs. Cyclic voltammograms of nitrophenolthiol and octadecanethiol suggested that a combination of polycrystalline gold and the use of PBS as an electrolyte caused excessive hydrogen evolution which overlapped with the reductive desorption peaks thus, generating high currents and unrealistic charge densities.

Acknowledgments

First of all I would like to thank Professor Jon Preece and Dr. Paula Mendes for giving me the opportunity to do my masters and for their continual support and dedication throughout my course. I have learnt a great deal about research and gained invaluable skills under their supervision. I am very grateful for their patience, guidance and encouragement in completing my thesis and I truly look forward to working with them in my PhD studies.

I would also like to thank Paul Yeung for his patience and commitment in supervising me throughout my masters; he took a significant amount of time out from his schedule to equip me with the practical knowledge that will no doubt set me in good stead for my future work in research.

I would like to thank everyone in the Preece and Mendes research groups for their advice and help during my research.

Finally I would like to thank my fiancée, Shelina, for her support and encouragement throughout my write-up. She has been an inspiration for me to always aim higher and do everything with excellence.

Abbreviations

CD	Cyclodextrin
CV	Cyclic voltammetry
ECM	Extra-cellular matrix
FEML	Fully extended molecular length
KKKKC	Lysine-Lysine-Lysine-Lysine-Cysteine
LD-SAM	Low density self-assembled monolayers
MHA	Mercaptohexadecanoic acid
NPT	Nitrophenolthiol
ODT	Octadecanethiol
OEG	Oligoethylene glycol
PBS	Phosphate buffer saline
SAM	Self-assembled monolayer
SCE	Standard calomel electrode
SPR	Surface Plasmon resonance
TEGT	Trielthylene glycolthiol
XPS	X-ray photoelectron spectroscopy

Contents

1   Introduction

1.1   Self-assembled monolayers

Self-assembled monolayers (SAMs) are films that form spontaneously onto a solid substrate via the adsorption of a surfactant. The basic molecular structure of SAMs (figure 1.1.) consists primarily of three components: a headgroup, backbone or chain and an endgroup. [1] SAMs are chemically bound to the surface via chemisorption due to a specific affinity for the substrate surface. The packing and degree of order in which the SAMs form mainly depend on the backbone which connects the headgroup and endgroup. The ease in which the properties of SAMs such as thickness, structure, surface energy and stability can be controlled[2] make SAMs a versatile field of research.
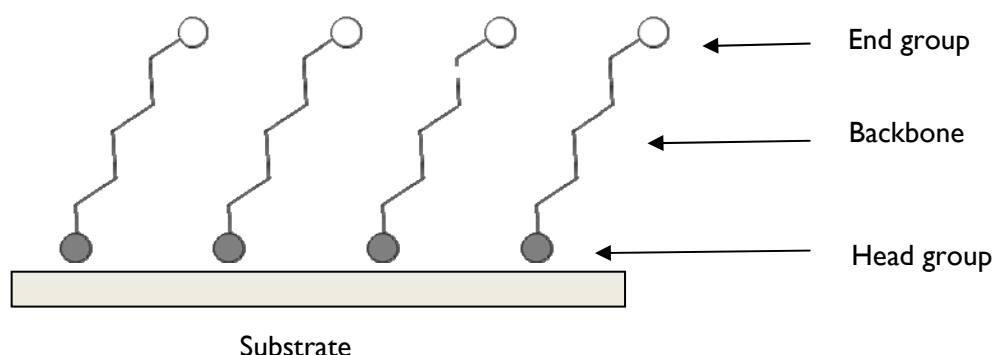
Figure 1.1. Schematic of the structure of SAMs

1.1.1   Surfactant

The headgroup binds strongly to the surface of a substrate via chemisorption. The choice of headgroup will depend on the substrate as different headgroups have varying affinities for substrates. The backbone has a number of important characteristics which affect SAM formation such as molecular ordering and the thermal stability of SAMs.[3] The length of the backbone in particular has an effect on the molecular ordering of the SAMs. Depending on the molecules, SAM formation with regard to the backbone can occur at a tilt angle

(as shown in figure 1.1.) especially in the case of alkanethiolates which are known to form well-packed SAMs.[2]

The endgroup is the key in determining the surface properties of the SAMs. Hence properties such as wettability[4] and bio-molecule immobilisation[5] may be modified. Switchable endgroups have recently been developed which respond to external stimuli, thus allowing for dynamic control of the surface properties (see section 2).

The affinity of the SAM for the substrate will vary in degree, depending on the headgroup and substrate. The most common types of SAMs are thiols on gold [6] and silanes on silicon dioxide (SiO_2).[7]

1.1.2 Thiol SAMs

Sulphur based SAMs have been shown to bind strongly to a range of metal surfaces including gold, silver, copper and platinum.[2] Gold has been the most commonly studied from among these substrates, as gold does not have a stable oxide[8] and so a clean gold surface can be handled in ambient conditions (see figure 1.2).[2]
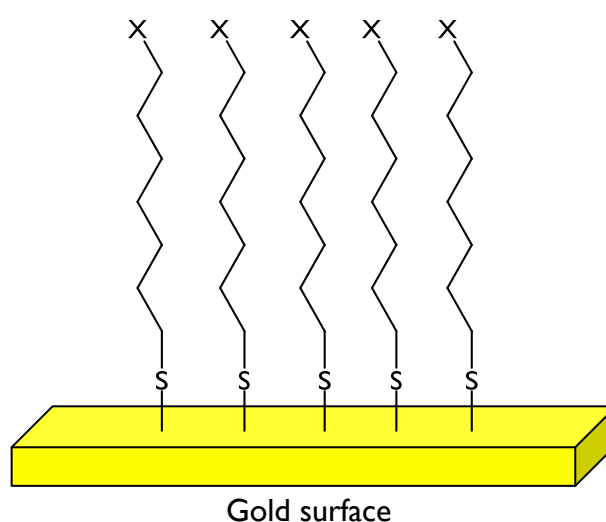
Gold surface

Figure 1.2. A monolayer of thiol SAMs on gold

The formation of alkanethiolates on gold can be described as an oxidative addition of the sulphur-hydrogen bond to the gold surface, followed by a reductive elimination of the hydrogen.

$$\text{R-S-H} + \text{Au}_n^0 \rightarrow \text{R-S}^-\text{Au}^+ \, \text{Au}_n^0 + \tfrac{1}{2} \, \text{H}_2$$

The thiolate (RS$^-$) adsorption has been proven to take place via XPS[9] and IR.[10] The bonding of the thiolate group to the gold surface is also very strong, approximately 40 kcal mol^{-1}.[3,11]

The immersion of a substrate in diluted thiol solutions of 0.1- 1 mM showed that the formation of alkanethiol monolayers on gold occurs over a two step kinetic adsorption process.[2] The initial process occurs rapidly, requiring a few minutes to reach 80-90% of the final thickness and surface coverage. The final process takes several hours to reach completion, where the SAMs reach their final thickness.[12] The rate at which the initial SAMs formation occurs is related to the length of the backbone, which means longer backbone chains have greater van der Waals interactions and thus their films form more rapidly than those of shorter chain molecules.[2]

1.1.3 Silane SAMs

Although there has been a great deal of focus on thiol based SAMs on gold, alkylsilane derivatives such as RSiX$_3$, where X is chloride or alkoxy and R is a carbon chain, are also known to form monolayers on hydroxylated surfaces such as silica.[2] Silane SAMs are less ordered than thiols on gold;[13] however, the stability of silane SAMs is greater than in thiol based SAMs both chemically and thermally.[14]

In the case of silane SAMs, water is adsorbed on to the surface in order to hydrolyse the silane molecules which then undergo condensation reactions with the surface hydroxyl groups.[15] Furthermore the hydrolysed silane SAMs form a polymerised network of

molecules, which are all covalently bonded to the surface. The adsorption process occurs via the silicon–chloride or silicon-alkoxy bond, which reacts with hydroxide groups on the surface of the substrate, hence forming a complex of silicon–oxygen–silicon bonds.[2,7] Overall there is an enhanced stability in silane SAMs compared to thiols on gold, primarily due to stronger binding and irreversible cross polymerisation between silane headgroups as shown in figure 1.3.[16]
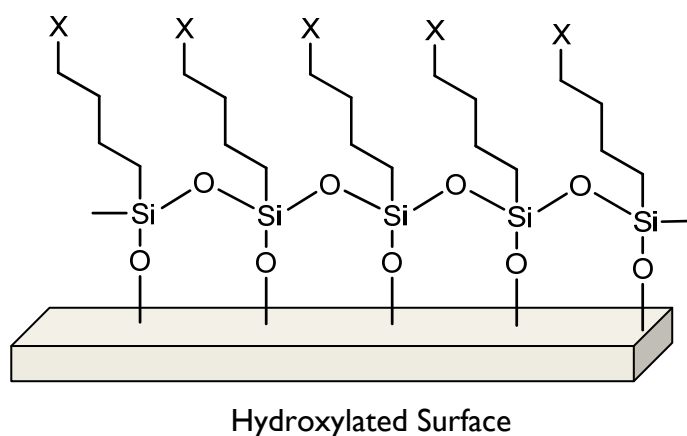
Figure 1.3. Alkanesilanes on hydroxylated surface

Despite the greater stability of silane SAMs, the process of producing high-quality silane SAMs has proven difficult due to the need to control the amount of water in solution and temperature.[17] On the other hand the absence of water results in incomplete formation of monolayers.[18]

1.1.4 SAM formation

The initial process in SAM formation is the physisorption of the molecules on to the surface. Physisorption consists of weak van der Waals forces between the SAM and surface of the substrate. An example is decanethiol on a gold (111) surface where the physisorption energy is in the region of 104 kJ mol^{-1}.[1] The example in figure 1.4 shows the formation of decanethiols on gold.

The real driving force behind SAM formation is chemisorption. Chemisorption occurs when the active headgroup of the surfactant adsorbs on to the substrate. The pinning of the headgroup on to the surface substrate is the most exothermic process, after which the SAM is adsorbed to the surface via a strong chemical bond to a specific site.

An example of the chemisorption process is the covalent Si-O bond in the case of alkyltrichlorosilanes on hydroxylated surfaces. Chemisorption for alkanethiols on gold occurs via the gold-sulphur bond.[2] These chemical bonds result in the ordering of SAMs over a period of time. The quality of SAM formation can be hindered by a number of factors such as contaminants on the surface and contaminants in solution.[19]
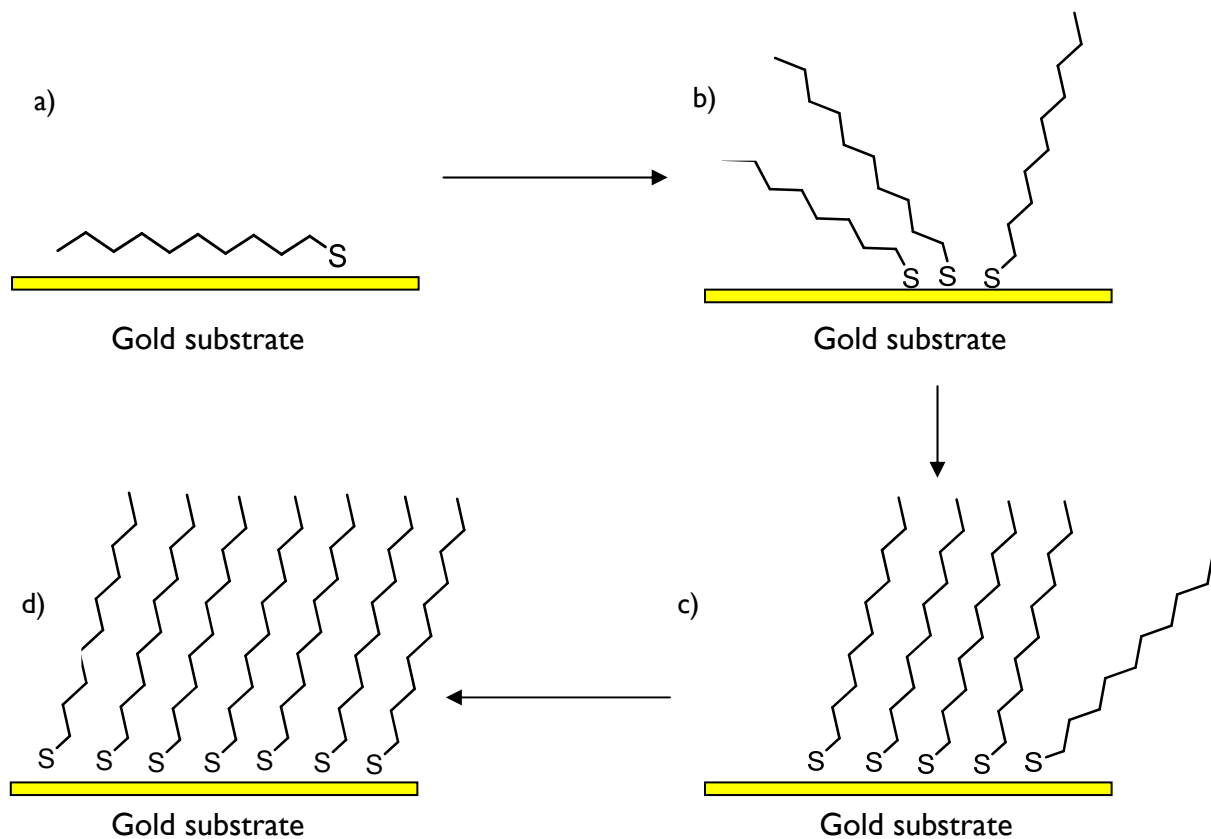
Figure 1.4. *Schematic showing the processes of SAM formation with decanthiol SAMs from a) SAM is physisorbed on to the surface by van der Waal forces, b) the SAMs are chemisorbed to the gold surface by strong covalent sulphur-gold bonds, c) the SAMs begin to form ordered monolayers and d) SAMs have formed fully ordered monolayers.*

The formation of SAMs is essentially a two-step process. The first process of physisorption of the surfactant on to the surface occurs within minutes of the substrate being immersed into a solution of surfactants. The surfactant at this stage lies parallel to the substrate via physical forces. The second process, known as chemisorption, begins within minutes and reaches completion at around 24 hours. The final process involves the ordering of the SAMs via dispersion interactions, which eventually form monolayers.

1.2   Mixed thiol SAMs

The use of mixed monolayers[14] is a more complex process than forming a single SAM. One of the uses for mixed monolayers is in creating a greater spatial distribution between SAM molecules. This can be achieved by selectively changing the endgroup functionality subsequent to SAM formation or by co-adsorbing two or more species onto the substrate during SAM formation. Co-adsorption is more widely used as it is still possible to control the final molecular composition and order of the SAM.[14] Previous studies of mixed SAMs suggest that the composition and surface coverage of the monolayer can be influenced by intermolecular interactions, the solvent and the surface during SAM formation.[20, 21]

The ability to produce specific molecular recognition systems using mixed biotinyl-functionalised monolayers has been exploited to immobilise neutravidin and streptavidin onto biotin successfully.[21,22] These systems have been important in the development of protein immobilisation on surfaces and as immunosensors.[22-59]

1.3   Protein inert surfactant

Research has been carried out in finding molecules that prevent non-specific binding of proteins, as they have a tendency to physically adsorb on to a substrate even without a specific binding site. This can be problematic because it significantly reduces the effectiveness of biosensors, molecule detection and single cell analysis.[23]

Oligoethylene glycol (OEG)-terminated SAMs have been used for numerous biological applications due to their ability to resist protein adsorption.[24, 25] It has been shown that OEG SAMs have high surface coverage and are able to prevent nonspecific protein adsorption.[23] Thus, OEG terminated SAMs are used commonly in diluting protein immobilisation surfactants, i.e. by the formation of mixed monolayers of OEG and a surfactant that has a reactive site that interacts with a specific moiety of the protein to be immobilised. By dilution it is possible to control the overall spatial distribution of proteins on the surface. A sufficiently spatially distributed surface will mean that the immobilisation of proteins is specific and not affected by any neighbouring protein molecules. A primarily protein-inert surface will allow for proteins to be immobilised in an accurate manner and thus, it is possible to study the desired cell protein interactions.[5]

1.4   Dynamic SAMs

Dynamic SAMs are monolayers which have a switching functionality; this provides them with an on/off mechanism. Compared to previous static extra-cellular matrix (ECM) models (see section 1.7), dynamic SAMs provide a new means to study how cells respond to changes in their environments in real time, thus offering a new method of studying cell migration.[5]

1.5   Switchable biological surfaces

Switchable surfaces that are responsive to external stimuli have been of great interest over recent years.[26-29] The ability to alter surface properties accurately in a controlled manner by way of an external stimulus has many potential uses such as biosensors, microfluidic chips, drug release systems and computers.[30] Recent developments in switchable surfaces have meant that properties such as wettability can now be modified using photochemical,[31-34] electrical,[4,35,36] solvent,[37,38] temperature[39] and pH control.[40-42] Essentially, switchable surfaces are SAMs or polymer based surfaces with the capacity for conformational changes upon the application of an external stimulus[43] thus, resulting in the simulation of an "on/off" switch as shown in figure 1.5.

External Stimulus
Thermal
Chemical
Electric
Optical

Bio-active (On)   Bio-inactive (Off)
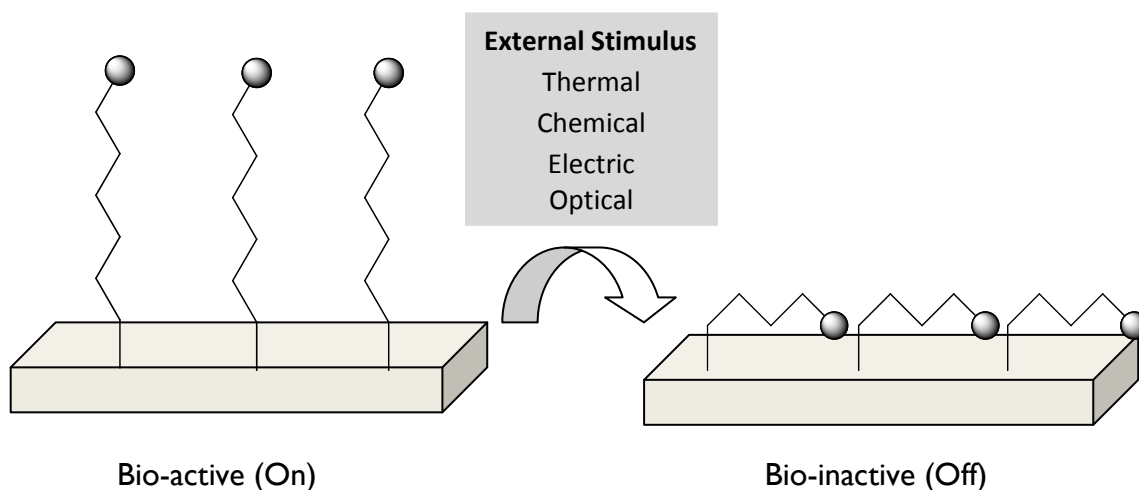
Figure 1.5. *Schematic illustrating the different types of external stimuli that can be used to alter the conformation of SAMs or polymer from bio-active to bio-inactive states. This allows for the control of biomolecule interactions on the surface.*

1.6   Stimuli responsive surfaces for biological applications

SAMs have proved to be an effective method of studying in-vitro biomolecule interaction. Molecular interactions occurring at biomolecular monolayer surfaces can be studied using a number of different analytical techniques such as surface plasmon resonance (SPR),[44] scanning probe microscopies[45] and also electrochemical techniques such as cyclic voltammetry (CV).[42]

Many of the systems being studied currently are an attempt to mimic properties of biological systems in order to reproduce biomolecule activity,[46] protein immobilisation,[28,36,47] cell adhesion and migration[48] at the solid-liquid interface. The applications for such surfaces could bring about many new benefits to the biological and medical fields.

1.7   ECM substratum models based on SAMs

Cells present in tissues interact with other cells through an extra-cellular matrix. The ECM is very complex and even until now it is not fully understood. The possibility to recreate the ECM model which will retain some of the characteristics of an actual ECM is very likely.[26] Surfaces that can reproduce an environment where the ECM model is applied will mean that research carried out on cellular interaction will be much more systematic than in the past. This will allow for the study of ways cells sense, integrate and respond to changes in the environment.[26]

The use of SAMs as a novel ECM model allows for cell attachment and migration via a specific, well-defined and controlled method. One of the main advantages in using SAMs in these models is that many important details are known about the environment such as thickness of SAMs, interchain distances etc. and thus they can be adjusted as required. This

high level of precision enables the isolated study of the desired protein-biomolecule interaction.

Currently protein immobilisation on SAMs is still a relatively new field whereas DNA immobilisation is well established. One problem is non-specific binding, which is the occurrence of unwanted protein binding that occurs at the surface of the SAMs via hydrogen bonding and hydrophobic interactions.[60]

Numerous methods of external stimuli have been used in order to control the properties of SAMs as mentioned in section 1.5. One of the most studied external stimuli is the use of electricity to control surfaces,[49] which have been successfully used to manipulate interactions of cells,[46,48] peptides,[48] DNA,[50,51] and proteins.[47]

The application of an electrostatic field near biological macromolecules can result in two different types of mechanisms: Faradaic processes, which involve electron transfer (redox chemistry) and non-Faradaic processes, which include changes to protein conformation, ion binding and protein-protein interactions.[49] Faradaic reactions are useful because they can give an indication of the electronic configuration of the protein and the reaction mechanism,[52,53] hence there has been numerous review articles written in the field of redox-active species.[53,55] The field of non-Faradaic reactions still remains for the most part unknown, until recently.

The study of protein adsorption on to electrode surfaces has previously been limited in its progress due to protein-electrode distances and protein denaturation upon adsorption. With the development of protein-attachment methods, SAMs and protein engineering techniques have made it feasible for the surface attachment of proteins with a significant level of activity.[55,59]

1.8   Electrically switchable surfaces

The development of switchable surfaces which can be controlled by means of an applied electrical potential has proven to be an effective tool and has been reported in many instances.[4,26,28,39] An example of electrochemically controlled immobilisation of DNA[54] and proteins[47] is by the use of aromatic nitro (NO_2) groups that were chemically modified via a redox process to amino (NH_2) groups. Mendes *et al.*[47] were able to demonstrate that the NO_2-terminated groups in the SAMs of 4-nitrophenol on gold surfaces could be reduced electrochemically and selectively to NH_2 groups by applying a negative potential across the functionalised electrode and its counter electrode in the presence of an electrolyte. By utilising a homo-bifunctional activated ester link, proteins were immobilised with high affinity and selectivity onto the NH_2 regions after activation.

Conventionally SAMs have been shown to be densely packed and so switching has not been possible, thus the need for low-density (LD) SAMs. An example of such a switchable surface can be found in the work done by Lahann *et al.*,[4] which was carried out using mercaptohexadecanoic acid (MHA) LD- SAMs to demonstrate reversible switching via an electrical potential (figure 1.6). A hydrophobic chain of MHA capped by a hydrophilic carboxylate group was used to allow for changes in surface properties. A space-filling end group was used to provide sufficient spatial distribution for each molecule to undergo a conformational change between "straight" and "bent". After the SAM formation cleavage of the space-filling end group presented a LD-SAM of MHA; conformational change in the MHA LD-SAMs was confirmed by the wettability of the surface being altered from hydrophobic to hydrophilic due to an electrical potential. These studies demonstrated a reversibly controllable switchable surface that can be formed with the use of a low density monolayer and electrical stimulus.
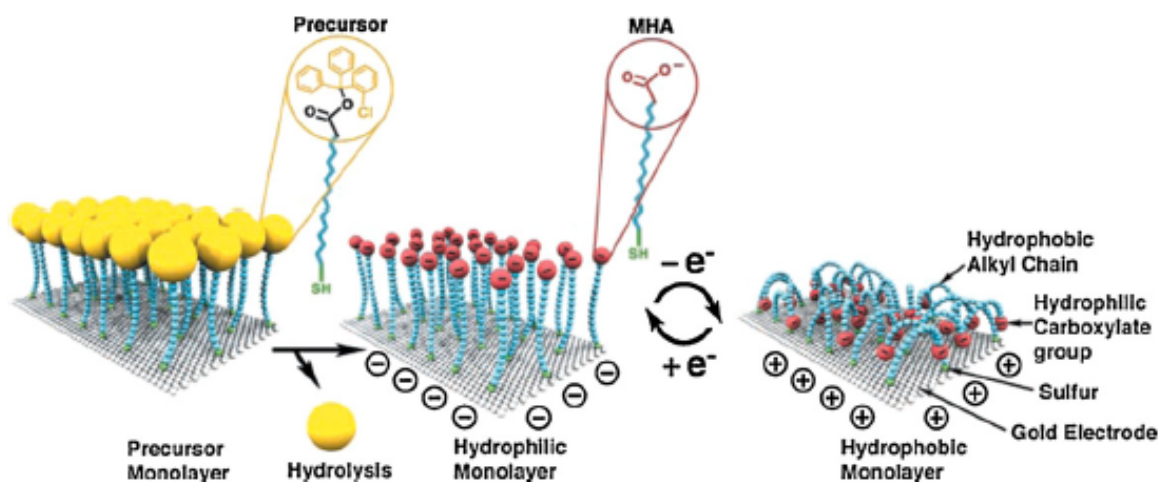
Figure 1.6. *Schematic showing the formation of LD-SAMs by utilising a bulky head-group, thus creating a monolayer which switched between hydrophilic and hydrophobic states upon the application of an electrical potential.*[4]

Further work was carried out on MHA using cyclodextrin (CD),[35] which wraps around the alkane thiolate, thus forming SAMs that have inherently low density. The CD can be unwrapped easily with a suitable solvent and as a result present reversible switching properties.[28]

Figure 1.7 represents a schematic of LD-SAMs that are reversibly switchable and showed observable changes in wettability, which can be determined by contact angle measurements. In addition the LD-SAMs prepared using this method were successfully utilised to bind fluorescently labelled avidin selectively.[35]
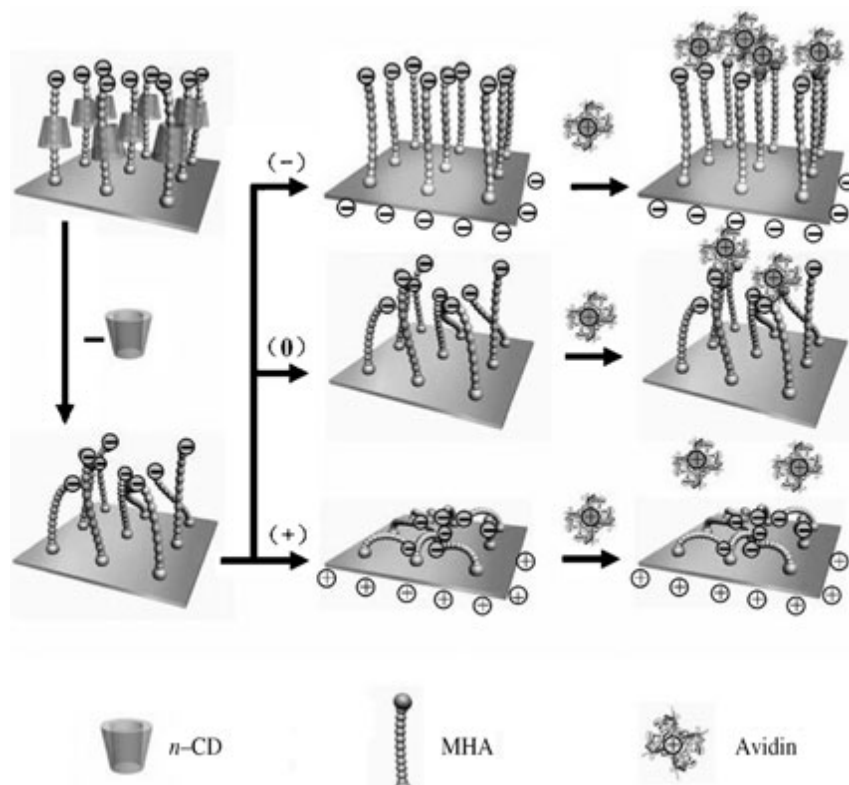
Figure 1.7. *Schematic showing the preparation of LD-SAMs and the conformational transition for MHA molecules at an applied potential. At negative potentials avidin binds to the surface and at positive potentials avidin does not bind to the surface.*[35]

Kong *et al.*[36] created a switchable surface using a microfluidic chip. By using LD-SAMs they showed that the application of an electric potential caused reversible conformational changes on SAMs with terminal carboxylic and amino groups. In this system they were able to control two types of protein adsorption to the surface, avidin and streptavidin using an electrical potential (figure 1.8). A carboxylic acid functionalised microfluidic chip was used to adsorb the positively charged avidin and upon the application of a positive potential the avidin was released. An amino-functionalised microfluidic chip was also used to adsorb negatively charged streptavidin and under a negative potential the protein was released. The switchable SAM surface was also used to separate a mixture of the two proteins thus,

showing potential uses as a controlled "on-chip" for capture of target proteins directly from a complex protein mixture.
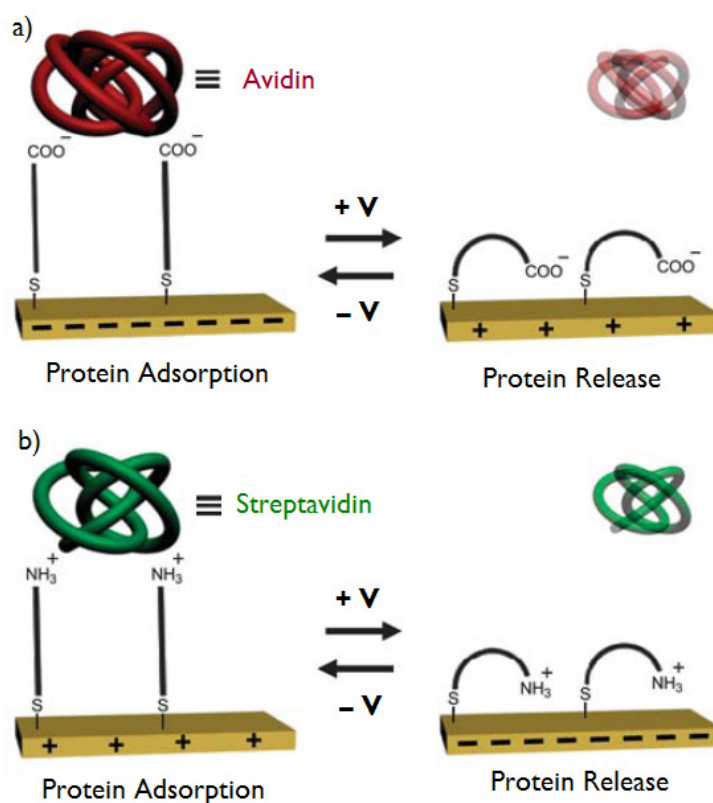
Figure 1.8. *Electrically controlled adsorption of avidin and streptavidin proteins using LD alkanethiolate SAMs on gold surfaces. (a) Carboxylic acid terminated and (b) amino terminated monolayers have shown reversible switching in conformation under a positive and negative potential.*[36]

Recently switchable peptide monolayers have gained recognition in the fields of biomedicine and biotechnology.[57] Functionalised alkanethiol monolayers form well-packed SAMs; as a result there is a size mismatch between the alkyl chain and the functionalised head-group, thus the need for peptide monolayers which can mimic the ECM and biomolecular interactions have been developed. This has led to the discovery of helical peptide-based monolayers, which possess a disulfide group on one side that anchors the molecule to the surface and a functional group on the other side.[57]

2 Instrumentation and characterisation techniques

The primary characterisation techniques used in this project were X-ray photoelectron spectroscopy (XPS) and ellipsometry. In order to study the stability of the peptide mixed SAMs, cyclic voltammetry was used to determine the potentials at which the SAMs were stable via reductive desorption studies. Fluorescence microscopy was also used to record any changes on a visual level that may have occurred due to an applied potential to the SAMs.

2.1 X-ray photoelectron spectroscopy (XPS)

XPS is a well known surface chemical analysis technique that can analyse the elemental composition which is present within a material. Essentially XPS works by the irradiation of a sample with a photon of energy (*hv*), which penetrates the surface and excites a core level electron. When a core level electron exceeds the binding energy (E_B), the atom will emit an electron, which is detected by the electron spectrometer (figure 2.1). By analysing the kinetic energy (E_K) involved in the emission of an electron the following equation can be derived[61]:

$$E_K + ø = hv - E_B$$

Equation 1.

Where *ø* is the work function of the spectrometer and remains constant, *hv* refers to the photon energy usually in the form of monochromatic x-rays, E_K is the kinetic energy of the electron and E_B is the binding energy of the electron.
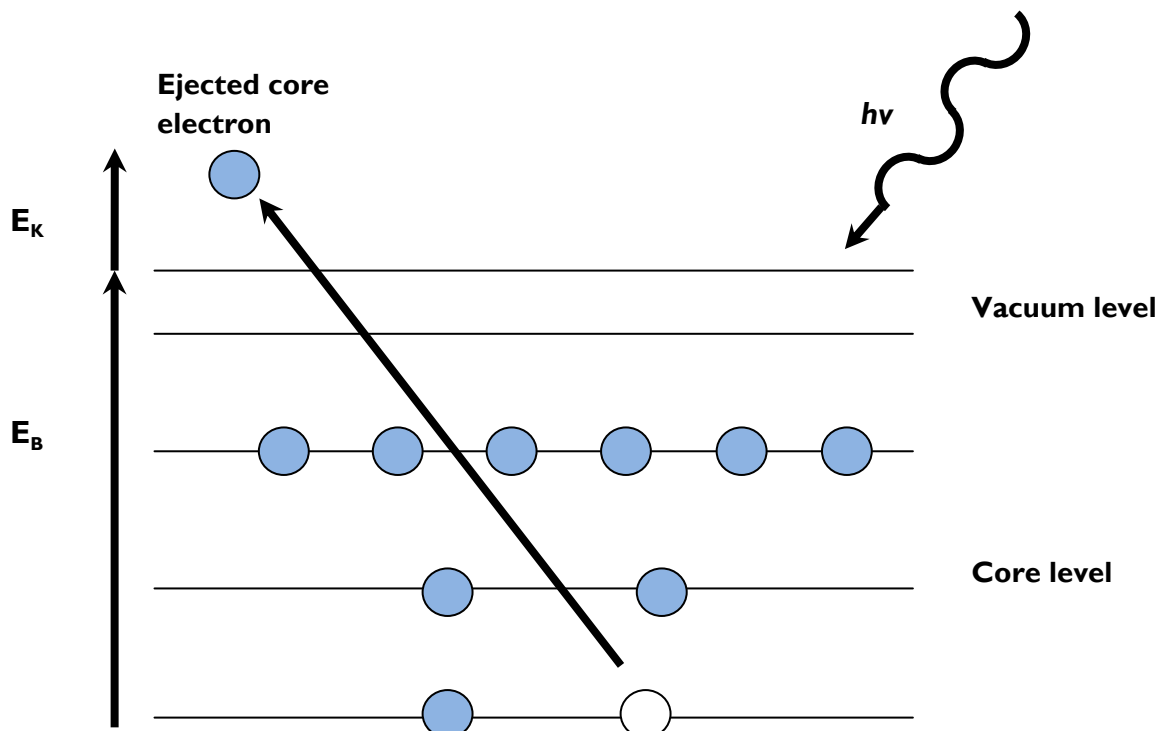
Figure 2.1. *Schematic of the XPS process, showing the photoionisation of an atom by the ejection of a core electron*

An XPS spectrum is a plot of the number of electrons detected versus the binding energy. Each element has a set of characteristic peaks at certain binding energy values, which can for the most part be relatively easy to identify after a sample is analysed. The binding energy differs from atom to atom and hence it determines the positions of the XPS peaks.

2.2   Ellipsometry

Ellipsometry can give valuable information about the formation of SAMs via thickness measurements. Ellipsometry works by the use of a plane-polarised light, which interacts with a surface at an angle. The light can be considered to comprise two components denoted s- and p-polarised.[2] The two components are then reflected from the surface with a different phase and amplitude. Finally when the s-and p- polarised light are combined once again they result in elliptically polarised light. This process allows ellipsometry to measure the thickness

between the surface of a substrate and air due to the ratio r between r_p and r_s, which are the reflection coefficients of the p- and s- polarised light respectively (figure 2.2).
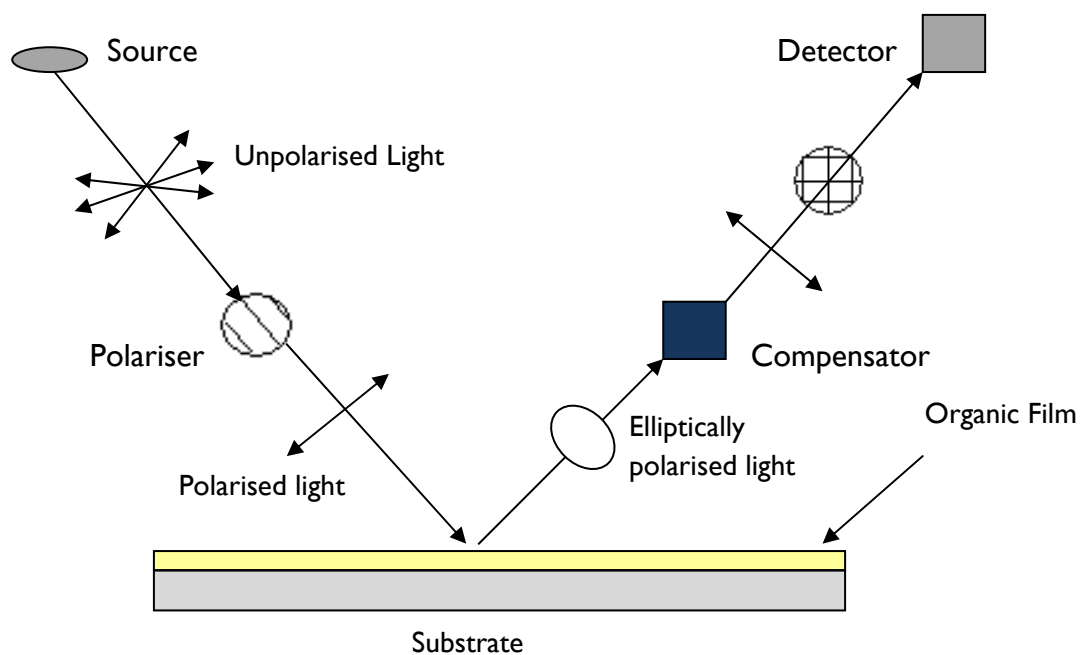
Figure 2.2. *Schematic of the mechanism of an ellipsometer*

2.3 Studying SAMs stability using electrochemistry

Electrochemical techniques such as cyclic voltammetry[62] and electrochemical impedance spectroscopy (EIS)[63,64] have been used to study the stability of SAMs on the solid-liquid interface. Cyclic voltammetry is commonly used in studying stability of SAMs due to its ability to detect defects within the SAMs, thus any inconsistencies can also be immediately pinpointed on a voltammogram.[65] Impedance measurements have also shown to be extremely sensitive to defects in a monolayer by giving information regarding the capacitance and ion double layer formation at the surface.[65]

2.3.1 Cyclic Voltammetry (CV)

Cyclic voltammetry is one of the most popular techniques used to study redox systems and the stability of SAMs. Essentially the electrode potential is scanned rapidly in search of redox couples by the sweeping of voltage between two fixed potentials at a fixed scan rate.[64,66] After the first potential is reached, the scan direction is reversed until it reaches the second potential and then finally again towards the initial potential. This process continues until the desired number of cycles has been reached.

A voltammogram is usually plotted with current against voltage to display the effects of the cyclic voltammetry on a sample. Analysis of a cyclic voltammogram provides numerous data that can be deduced about the SAM substrates, such as: reduction, oxidation, stability and consistency of monolayers in varying samples, desorption and surface coverage of a monolayer.[65]

A great deal of research has been carried out using the CV reductive desorption technique to determine the surface coverage of SAMs.[67-70] Reductive desorption occurs when an extreme cathodic potential is applied until the SAM on the surface is completely removed due to the level of electron transfer causing reduction and consequent removal of the SAM. An example reported in literature using dodecanethiol SAMs is shown in figure 2.3 where two clear reductive desorption peaks appear: the first at -1.00 V and the second at -1.18 V. Each corresponds to a different amount of energy required to reductively remove thiol molecules.
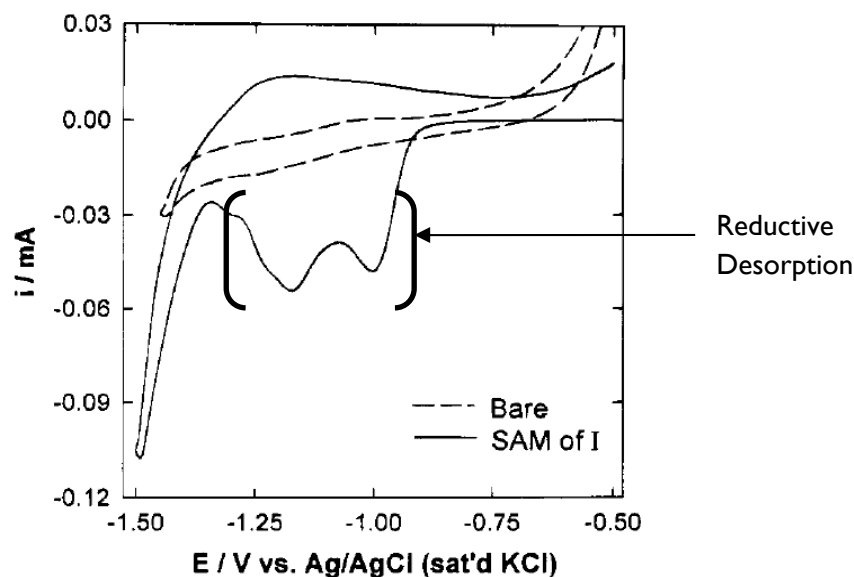
Figure 2.3. *Reductive desorption at 500 mV/s in 0.5 M KOH/ethanol vs Ag/AgCl (saturated KCl) of a bare gold electrode and gold electrode coated with dodecanethiol.*[67]

Lemay *et. al.*[71] were able to demonstrate reductive desorption using a mixed monolayer of 2-aminoethanethiol (AET) and 11-mercaptoundecanoic acid (MUA) on a polycrystalline gold bead electrode. During the negative potential sweep of the curve it is possible to observe the different desorption peaks of the AET from the (111), (100) and (110) faces of the polycrystalline gold surface (Figure 3.4).
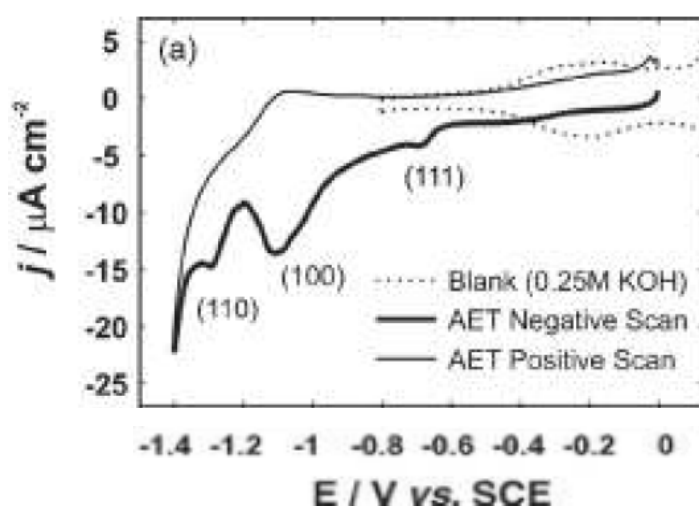
Figure 2.4. *Reductive desorption at 25 mV/s in 0.25 M KOH vs SCE of AET modified gold electrode.*[71]

2.4   Fluorescence Microscopy

Fluorescence microscopy illuminates organic or inorganic specimens with light of a specific wavelength, which is absorbed by the fluorescently labelled specimen, also known as a fluorophore. The light causes the fluorophores to emit longer wavelengths of light, thus allowing for the observation of physical changes on a monolayer. Any other form of light is separated from the much weaker emitted fluorescence through the use of an emission filter.[72] Fluorescence microscopy is commonly used to observe selective binding of fluorescently labelled proteins such as neutravidin,[73] streptavidin[74,75] and avidin[36] onto biotinylated SAMs.

3   Aims and Objectives

3.1   Overall aim

The long term goal of this project is to achieve a spatially distributed monolayer of mixed SAMs using biotinylated oligolysine peptide (Biotin-KKKKC) and triethylene glycolthiol (TEGT) that can be used to selectively bind protein to the surface via an on/off mechanism. The on/off mechanism in this project is in the form of an electric potential (see figure 3.1).
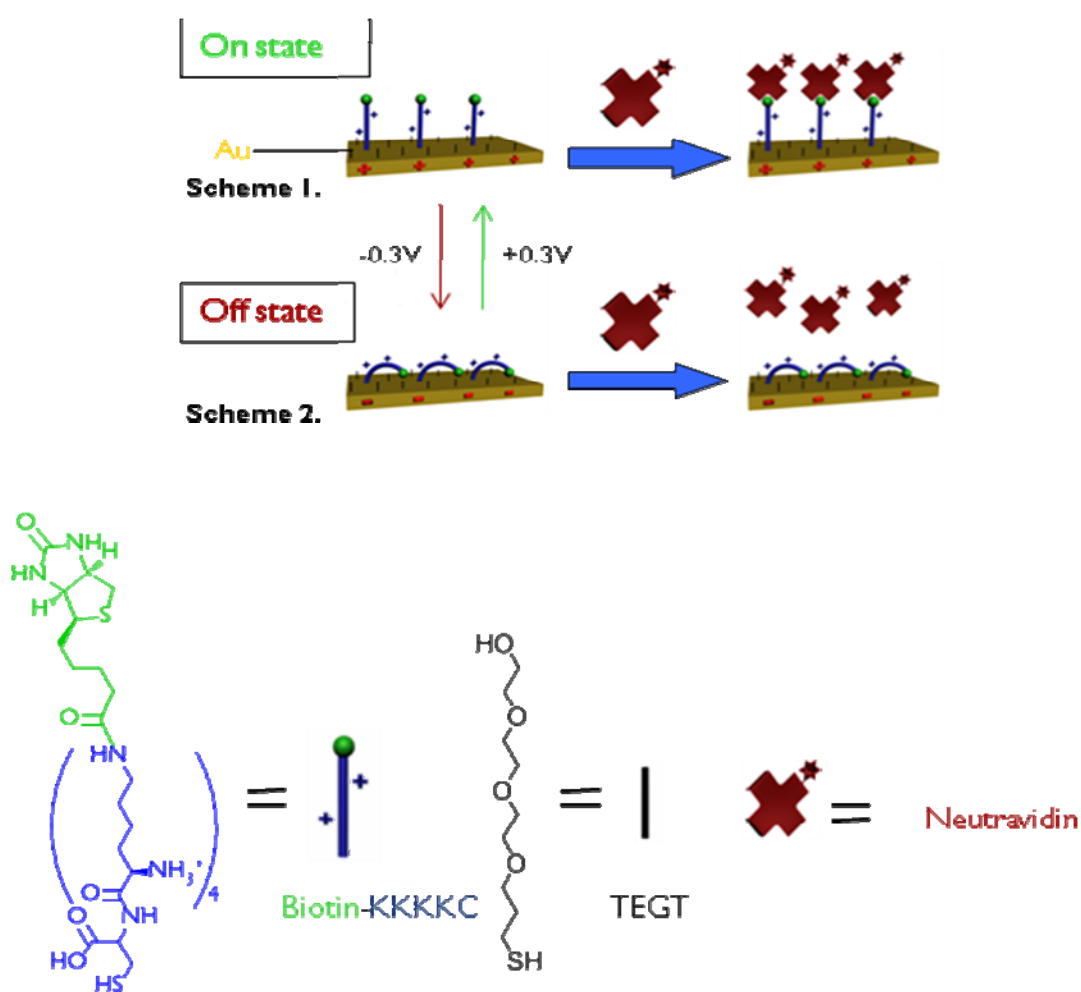
Figure 3.1. *Scheme 1 represents the mixed SAMs in an on state where the biotinylated peptide is in a stretched conformation, hence binding occurs. Scheme 2 shows the biotinylated peptide concealing the binding sites, thus protein binding does not occur or is reduced significantly.*

The oligolysinepeptides exhibit protonated amino side chains at pH = 7, providing the basis for the on/off switching of the biological activity on the surface. It is expected that when a positive electric potential is applied to the surface (scheme 1), the biotin peptide chain will be in a stretched out conformation, due to electrostatic repulsion. The stretched out conformation will leave the biotinylated exposed and hence the neutravidin will bind onto the available biotin binding sites. Conversely, when a negative potential is applied to the surface (scheme 2), it is expected that the biotinylated peptide will be electrostatically attracted to the surface, hence concealing the biotin binding sites. This would result in minimal or reduced neutravidin binding.

3.1.1 Optimising mixed monolayer ratio for switching

The mixed monolayer consists of TEGT and a biotinylated peptide. The biotin peptide that will be used consists of a cysteine group, four lysines and a biotin functional group (figure 3.1). The biotinylated peptide SAM will adsorb to the gold substrate via the cysteine group, which contains a thiol moiety that binds to the gold. The 4 lysine groups in the peptide chain will give the biotin-KKKKC enough manoeuvrability to switch conformations between the on and off states when a potential is applied.

The biotin end group is the key to the selective binding process that we seek to recreate. The primary use of TEGT is to help spatial distribution between the biotin-KKKKC, optimising the switching. TEGT was used due to its inert nature and inability to bind to protein molecules, thus reducing any non-specific binding.

By theoretical calculations it has been determined that the maximum possible area each peptide can occupy after a successful switch is 3 nm^2. The maximum molecular area was calculated based on the length of the exposed part of the peptide on the mixed SAM, i.e.

fully extended molecular length (FEML) of the peptide and FEML of the TEGT molecule. The calculated FEMLs of the peptide and TEGT are 4.7nm and 1.6 nm respectively, obtained with ChemiBio 3D Ultra 11.0 (figure 3.2). If it is assumed that the TEGT molecule has a footprint of $0.214nm^2$,[76] a ratio of 1 biotin-KKKKC peptide for every 15 TEGT molecules must be obtained on the surface.

It has been shown that the ratio of molecules in a mixed thiols solution is rarely identical to the ratio of the molecules on the surface.[77] In order to find the optimum mixed SAM solution ratio between biotin-KKKKC and TEGT, a range of samples will be investigated via XPS. By determining the ratio of nitrogen and sulphur atoms present in biotin-KKKKC and TEGT, an estimation of the number of molecules present on the surface can be made.
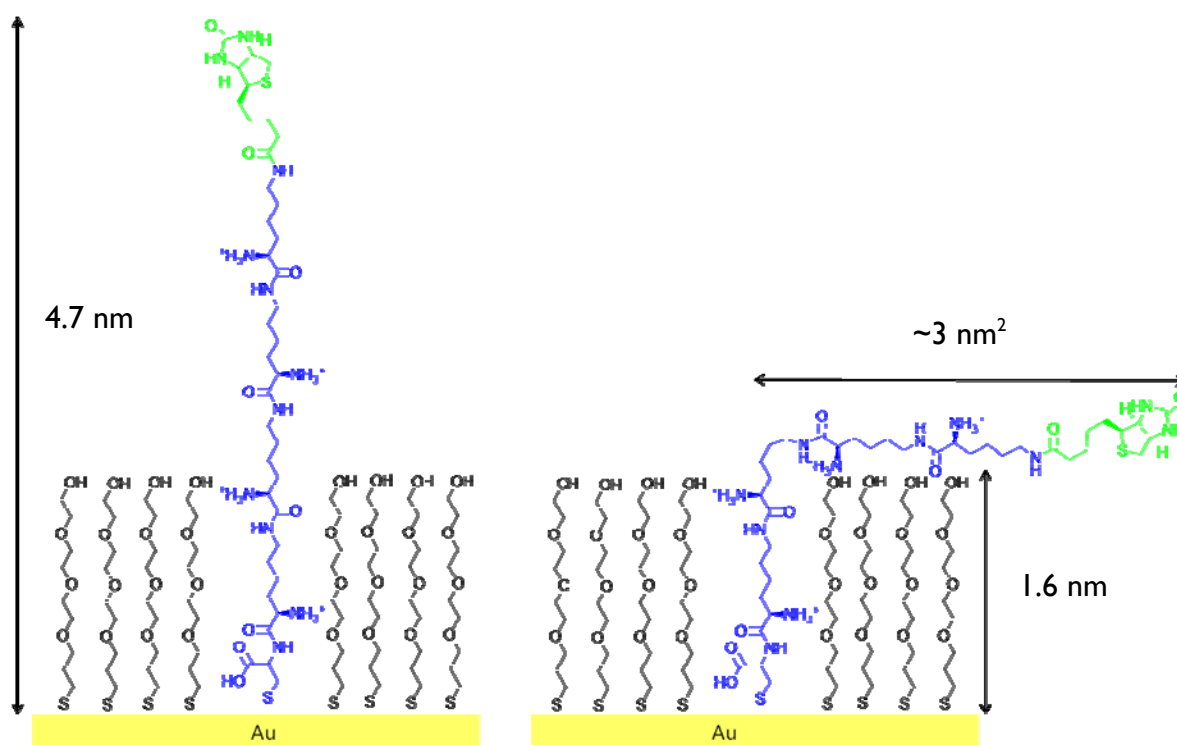
Figure 3.2. *Schematic of the length of the peptide SAM before and after switching.*

3.1.2 Measuring mixed SAMs thickness

In addition to XPS, ellipsometry will also be used in order to carry out thickness measurements on different samples. Thickness measurements will be compared to theoretical lengths of the molecules. This will give an indication into the conformation of the molecules on the surface.

3.1.3 Observing switching via fluorescence

In order to gain a visual observation of the switching, a preliminary study will be carried out using fluorescence microscopy. By fluorescently labelling the neutravidin it is possible to observe the contrast between the on and off states. The on state would show a brighter image due to increased neutravidin binding, whereas the off state would appear as a darker image due to less neutravidin binding. Brightness will be measured by a figure of image intensity.

Control experiments will also be carried out with a similar peptide SAM without the biotin (KKKKC) as shown in figure 3.3. This will help to ensure that binding of neutravidin is occurring strictly on the biotin binding sites. It is expected that no neutravidin should bind to the KKKKC mixed SAMs, but non-specific binding may occur. Non-specific binding is the occurrence of molecules binding to the surface through non-specific interactions (i.e. hydrophobic/hydrophilic and electrostatic interactions). The use of neutravidin should minimise non-specific binding because it is electrically neutral, hence the application of a potential should cause no electrostatic attraction between the neutravidin and the surface.
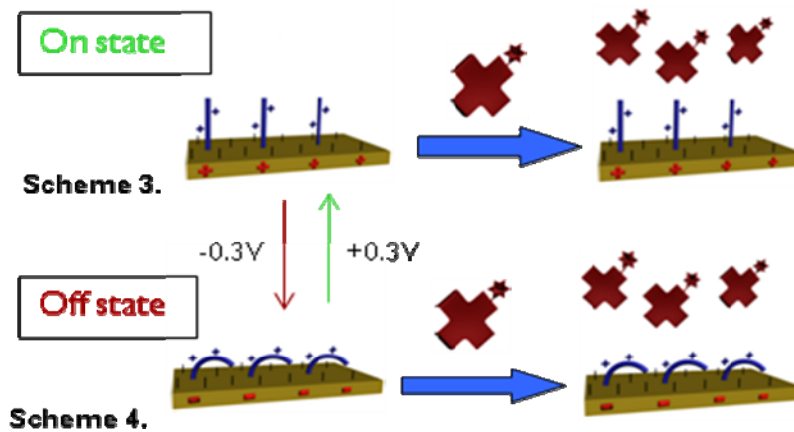
Figure 3.3. *Scheme 3 and 4 represents the peptide SAM without biotin. Both before and after applying a potential there is no binding, due to the lack of available binding sites.*

3.1.4   Studying stability and surface coverage

The main focus of this project will be the stability studies of the mixed SAMs using cyclic voltammetry (CV). CV is a useful technique in determining surface stability of SAMs and also for determining surface coverage. In these experiments the objective will be to carry out CVs on different samples of pure and mixed SAMs to measure the reductive desorption peak. The reductive desorption peak will give a value of charge density, which can be used to calculate the surface coverage and also the stability of the SAMs.

Initially a positive potential will be applied, where the film is stable and no oxidation is visible on the CV curve, then an extreme negative potential. The extreme negative potential will cause a partial or complete removal of the mixed SAMs.

By integrating the reductive desorption peak, the charge density and hence the surface coverage can be calculated. A consistent value for surface coverage between samples will indicate a stable monolayer is formed each time. A varied surface coverage will mean the formation of SAMs is not consistent.

This study will be divided into two parts:

1. CV will be carried out on samples which have had no applied potential beforehand. These will be known as the open circuit samples. The purpose of this set of experiments will be to check the consistency of the SAMs formation.

2. Samples which have been conditioned under an applied potential for an hour, thereafter CV will be carried out. This set of experiments will give an indication as to whether applied positive and negative potentials remove the SAMs from the surface. By comparing the surface coverage values of the open circuit samples and applied potential samples, it will be possible to quantify whether SAMs have been removed. This will also help to confirm whether any contrasts in image intensity from the fluorescence image studies were due to SAMs removal or switching.

4   Experimental

4.1   Materials and Chemicals

Commercially available chemicals and solvents were purchased from Aldrich Chemicals and Fisher Chemicals. Oligopeptides (Biotin-KKKKC and KKKKC) were synthetised by Peptide Protein Research Ltd. (Wickham, UK) to > 95% purity and verified by HPLC and mass spectrometry. Neutravidin and Alexa Fluor 568 Protein Labeling Kit were purchased from Invitrogen and used as received. Water was purified using a Millipore integral system.

TEGT was synthesised through a multistep route by Parvez Iqbal (figure 4.1). The commercially available triethylene glycol was alkylated with allyl bromide at reflux in basic conditions to obtain **1**. **1** was converted to **2** in the presence of thioacetic acid and AIBN heated at reflux for 1 h. Deprotection of **2** was performed in mild acidic conditions at reflux for 4 h to obtain TEGT.
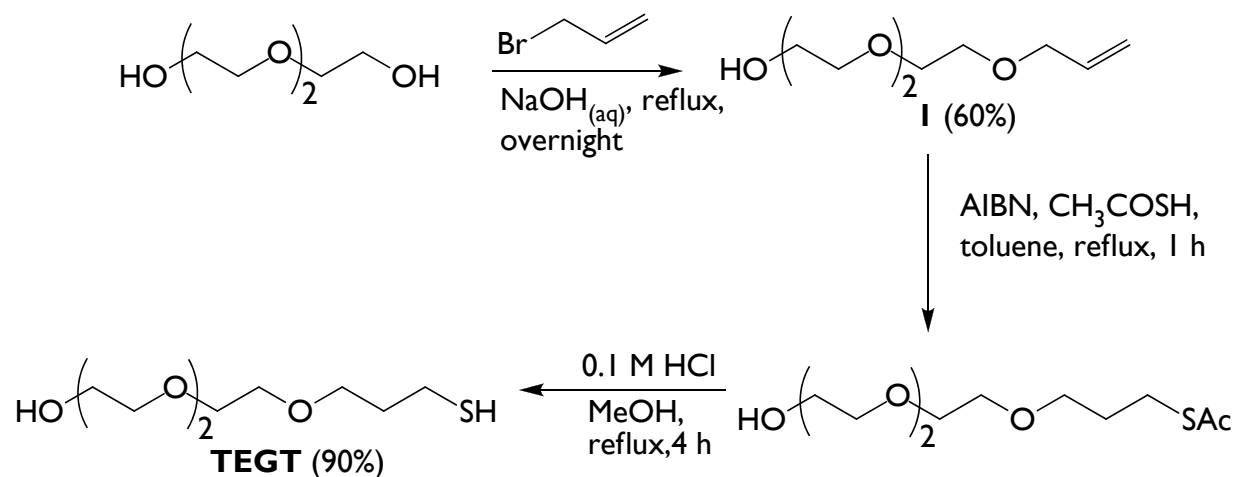
Figure 4.1. Synthesis of TEGT

4.2   Preparation of SAMs

Polycrystalline substrates were purchased from George Albert PVD., Germany and consisted of a 100 nm gold layer deposited onto a silicon wafer covered with a thin layer of titanium The gold (Au) substrates were cleaned by immersion in piranha solution (3:1, H_2SO_4 : 30% H_2O_2) at room temperature for 10 min, rinsing with Ultra High Purity (UHP) H_2O and then HPLC grade EtOH thoroughly for 1 min. (*Caution: Piranha solution reacts violently with all organic compounds and should be handled with care.*)[5] Solutions of the oligopeptide (1 mM) and TEGT (0.1 mM) were prepared in EtOH containing 3% (v/v) $N(CH_2CH_3)_3$, and mixed at the concentration ratio of 1:1, 1:5, 1:10, 1:40, 1:50 and 1:100. Subsequently, the clean Au substrates were immersed in the mixed solution for 12 h to form the mixed SAMs on the Au surfaces. The substrates were rinsed with an ethanolic solution containing 10% (v/v) CH_3COOH. Note that the mixed SAMs were deposited in the presence of $N(CH_2CH_3)_3$ to prevent the multilayer formation between the NH_2 functional groups of the bound thiolate peptide on Au surface and that of free thiol peptide in the bulk solution.[78] The same procedure was used for the preparation of pure biotin-KKKKC and pure TEGT SAMs as mentioned above.

4.3   X-ray Photoelectron Spectroscopy

XPS spectra were obtained on the Scienta ESCA300 instrument based at the Council for the Central Laboratory of the Research Councils (CCLRC) in The National Centre for Electron Spectroscopy and Surface Analysis (NCESS) facility at Daresbury, UK. XPS experiments were carried out using a monochromatic Al K_α X-ray source (1486.7 eV) and a take off angle of 15°. High-resolution scans of N (1s) and S (2p) were recorded using a pass energy of 150 eV at a step size of 0.05 eV. Fitting of XPS peaks was performed using the *Avantage* V2.2 processing software.

4.4 Ellipsometry

The thickness of the mixed SAMs was determined by multiwavelength spectroscopic ellipsometry. A Jobin-Yvon UVISEL ellipsometer with white light source was used for the measurements. The angle of incidence between the director and the polariser was set to 45°. The DeltaPsi software was employed to determine the thickness values using a Cauchy model. The thickness reported is the average of six measurements, each made at different points on the substrate.

4.5 Cyclic Voltammetry

Potential and time-dependent stability studies were performed using a Gamry PCI4/G300 with a custom-designed Teflon cell, equipped with the functionalised Au substrate as the working electrode, a Pt wire as the counter electrode, and a standard calomel electrode (SCE) as the reference electrode. The gold working electrode exposes a circular geometric area of 75.2 mm^2 to the electrolyte solution (figure 3.2).

Electrical potentials of + 0.3 V and − 0.3 V were applied for 30 min to the mixed SAMs in phosphate buffer saline pH 7.4 (PBS) solution. Subsequently, the mixed SAMs were analysed by CV in a PBS solution by sweeping the potential *in the negative* direction from + 0.3 V to −1.2 V and then to + 0.3 V at a scan rate of 50 mV/s. The PBS solution was purged with Ar for ~ 20 min prior to each measurement and kept under Ar during the course of the experiment. Similar CV measurements were performed on pristine mixed SAMs. The charge density reported is the average of five measurements.
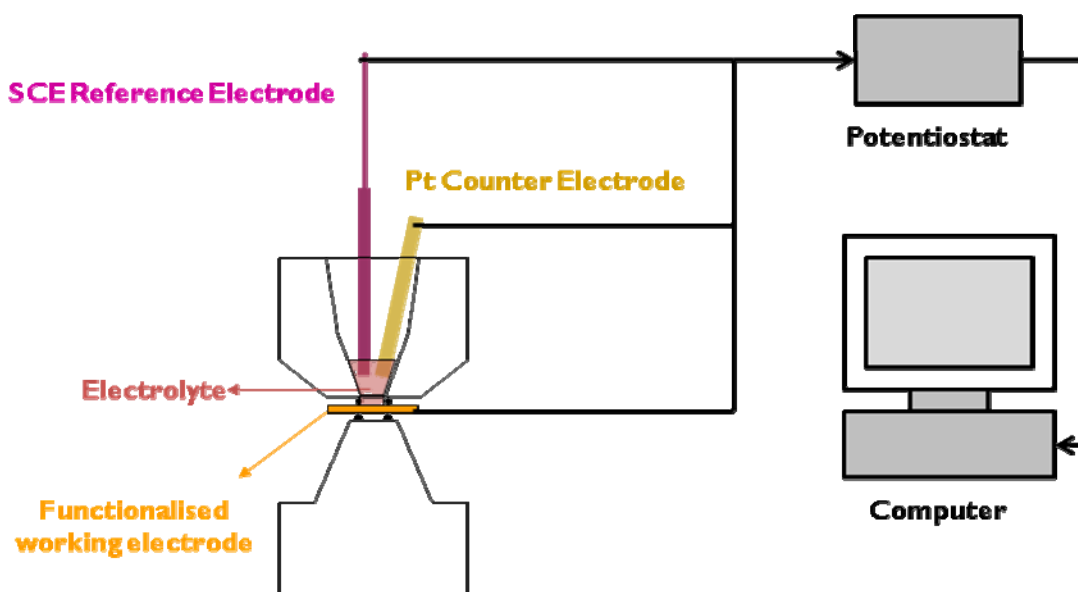
Figure 4.2 *Schematic of experimental used in cyclic voltammetry experiments*

4.6 Fluorescence Microscopy Switching Studies on Mixed SAMs

An electrical potential was applied to the mixed SAMs on Au using a Gamry PCI4/G300 with a custom-designed Teflon cell, equipped with the functionalised Au substrate as the working electrode, a Pt wire as the counter electrode, and a saturated calomel electrode as the reference. For the bio-active state (neutravidin-biotin binding), an electrical potential of + 0.3 V was applied for 10 min on the gold substrate in a 500 µl PBS solution, followed by the addition of a 500 µl PBS solution of the fluorescently-labelled neutravidin (74 µg ml^{-1}), whilst maintaining the + 0.3 V potential for a further 30 min in the dark. The substrates were rinsed with PBS for 10 min and mounted for fluorescence microscopy. For the bio-inactive state (neutravidin-biotin non-binding), the same procedure was used but instead of applying a positive voltage, – 0.3 V was applied.

4.7   Fluorescence Microscopy

Fluorescence images were collected on a Zeiss SM-LUX fluorescent microscope, equipped with a Canon Powershot G5 monochrome camera using a mercury lamp as the light source. Pictures were acquired using software remote capture with identical exposure parameters and analysed using *Image J 1.40g* (NIH). No postexposure image processing was performed.

5   Results and Discussion

5.1   Optimisation Studies of Mixed SAMs using XPS

XPS studies were carried out in collaboration with Chun Ling Yeung on numerous samples of pure and mixed SAMs. Mixed SAMs of biotin-KKKKC and TEGT were prepared at different solution ratios: 1:1, 1:5, 1:10, 1:20, 1:40, 1:50 and 1:100 in order to investigate the best possible mixed ratio of peptide and TEGT SAMs, which would allow for optimum switching of the peptide SAM. As mentioned previously, the solution ratio of molecules rarely reflects the same ratio on the surface due to preferential adsorption of one of the molecules.

High-resolution XPS spectra were acquired from samples to give a clear indication of the elemental composition of the SAMs and a ratio of nitrogen to sulphur. XPS confirmed the formation of pure and mixed SAMs. In figure 5.1 scans of the N (1s) region show the presence of nitrogen on the pure biotin-KKKKC SAMs and biotin-KKKKC:TEGT mixed SAMs from a 1:40 solution ratio. For pure TEGT there were no N (1s) peaks observed. As expected, as the solution ratio of TEGT increases in relation to biotin-KKKKC, the N (1s) peak area decreases.

The biotin-KKKKC peptide consists of 11 N atoms and 2 S atoms whereas TEGT has no nitrogen and only one sulphur atom. By integrating the area of the S (2p) and N (1s) peaks for the mixed monolayers, it was possible to calculate the ratio of biotin-KKKKC and TEGT on the surface. From a solution ratio of 1:40 of biotin-KKKKC:TEGT an average ratio of 1 biotin-KKKKC to 15 TEGT molecules on the surface can be expected (see figure 3.2).
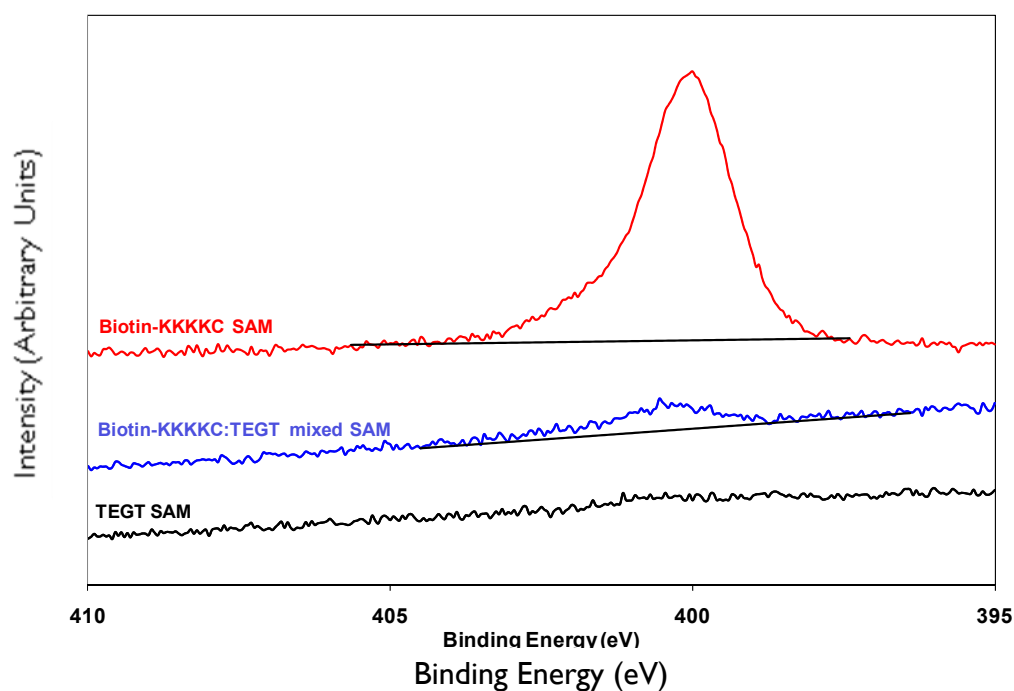
Figure 5.1. *XPS spectra of the N (1s) peak region of pure Biotin-KKKKC SAMs, pure TEGT SAMs and mixed SAM of the Biotin-KKKKC peptide and TEGT-terminated thiol from a 1:40 solution ratio.*

5.2   Mixed SAMs thickness by Ellipsometry

The successful functionalisation of the gold surfaces was also confirmed by ellipsometry. Ellipsometry was used to carry out thickness measurements on pure TEGT SAMs, pure biotin-KKKKC SAMs and mixed SAMs of biotin-KKKKC:TEGT at a ratio of 1:40. The monolayer thickness obtained for the pure TEGT SAMs and pure biotin-KKKKC SAMs (Table 6.1) are smaller than the molecular length of the molecules taken from ChemDraw 3D. Similarly the thickness of the mixed SAMs of biotin-KKKKC:TEGT at a 1:40 ratio is less than the calculated length of the molecules. The results obtained from the thickness measurements suggest that pure monolayers do not assemble in a stretched out conformation but rather in a tilted or lying-down phase,[79] leading to the formation of low density SAMs. The ellipsometric thickness of the mixed SAMs of biotin-KKKKC:TEGT at a

1:40 ratio is longer than that of the pure TEGT SAMs, but shorter than that of the pure peptide SAM, thus suggesting the presence of a mixed monolayer on the gold surface.

Mixed SAMs solution ratio	Calculated length of molecule (nm)	Thickness average (nm)
pure TEGT	1.6	0.653 ± 0.213
pure Biotin-KKKKC	4.7	0.926 ± 0.188
1:40	-	0.736 ± 0.207

Table 5.1. *Thickness measurements obtained using pure TEGT SAMs, pure biotin-KKKKC and a mixed SAM of biotin-KKKKC:TEGT at a 1:40 ratio. Calculated lengths were derived from ChemDraw 3D.*

5.3   Fluorescence Microscopy Switching Studies on Mixed SAMs

The primary use of fluorescence microscopy at this stage was to carry out a preliminary study of the biotin-KKKKC peptide switching. A contrast in image intensity between the positive and negative applied potentials would give an early indication of any switching that occurs.

Earlier work carried out by Kong *et al.*[35] using mercaptohexadecanoic acid (MHA) LD-SAMs indicated that a stable potential range for electrochemical studies with SAMs was between +0.3 V and -0.3 V; hence this potential range was followed through in this project as a starting point.

In order to understand the potential switching efficiency of the biotin-KKKKC peptide, an electric potential of +0.3 V or –0.3 V was applied to the gold surface with a mixed monolayer. Experiments were carried out in the presence of neutravidin for a fixed period

of time. Subsequently fluorescent images were taken to show the image contrast between the on and off states, as well as giving an indication of the amount of protein binding that had taken place on the surface.

Fluorescent images collected for an applied positive and negative potential to the surface (figures 5.3a and 5.3b) showed a significant difference in fluorescence image intensities, thus indicating that some switching has occurred. Fluorescence images from figure 5.3a suggest that neutravidin has bound to the surface, whereas in figure 5.3b it appears there is less neutravidin-biotin binding. In conclusion figures 5.3a and 5.3b suggest that there is less binding taking place during the application of a negative potential due to the significant reduced image intensity.
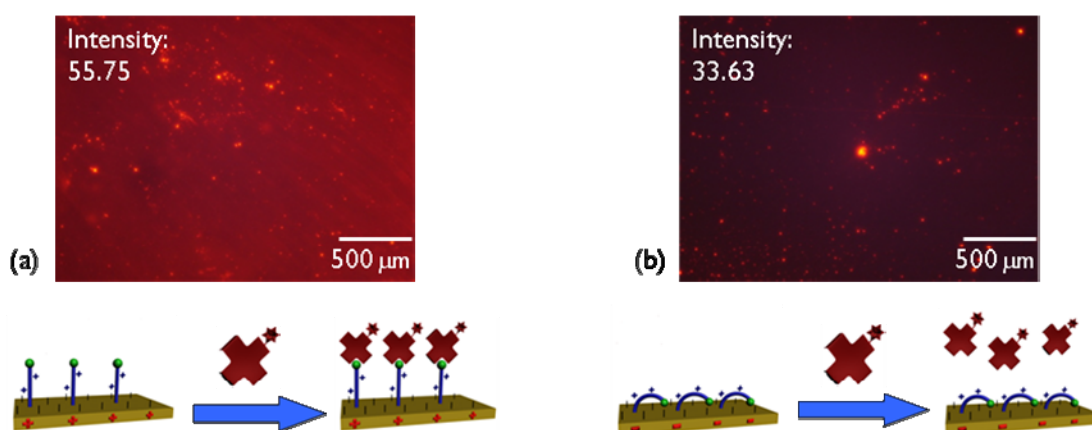
Figure 5.3. *Fluorescent images of a mixed SAM surface with biotin-KKKKC and TEGT after an applied potential of (a) +0.3 V and (b) −0.3 V in the presence of fluorescently labelled neutravidin*

The appearance of bright spots observed in fluorescence images shown in figure 5.3 indicate the possibility of protein aggregation, where a number of neutravidin molecules may have aggregated onto a single biotin. Another possibility for the occurrence of these bright spots could be due to island formation.[80] Island formation is a known phenomenon in mixed SAMs and can occur due to the presence of clusters of peptide binding sites (figure 5.4).
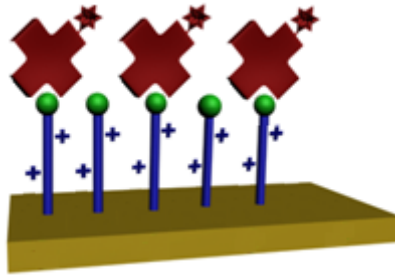
Figure 5.4. *Schematic of mixed SAMs with biotin-KKKKC in an island formation*

From XPS data the surface ratio of molecules of biotin-KKKKC and TEGT has been established, but the question still remains over the exact spatial distribution of these molecules in a fully formed monolayer. The biotin end group on the peptide chain and the TEGT will certainly help in the spatial distribution, but precisely to what extent is still unknown.

The application of a negative potential was a direct cause of the decreased fluorescence image intensity as shown in figure 5.3b. There could be two primary reasons why lower image intensity is observed due to a negative potential, which are as follows:

1. The biotin-KKKKC peptide has undergone a conformational change, thus concealing the biotin binding sites. Any other form of neutravidin binding to the surface may have occurred due to non-specific binding as explained in section 4.1.3. The only visible binding that has occurred appears in the form of bright spots and this may be due to isolated peptides that did not switch conformation and remained stretched out (figure 5.5).
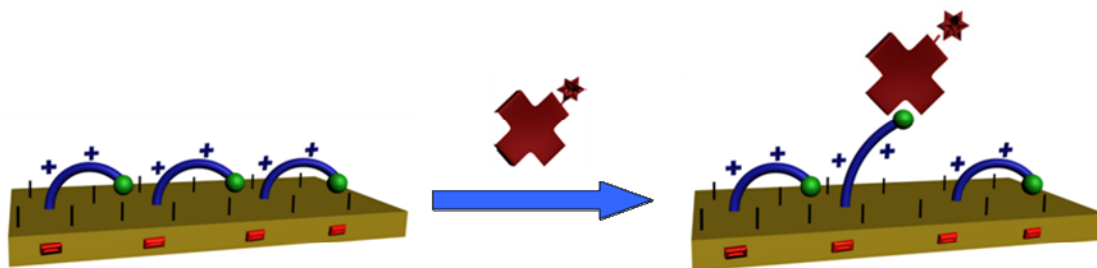
Figure 5.5. *Schematic of applied negative potential on surface with partial binding.*

2. The application of a negative potential to the gold surface caused the mixed SAMs to desorb, thus leaving fewer binding sites for the neutravidin. This would mean the majority of biotin-KKKKC molecules, which contain the biotin binding site had been desorbed from the surface due to the application of a negative potential (figure 5.6).
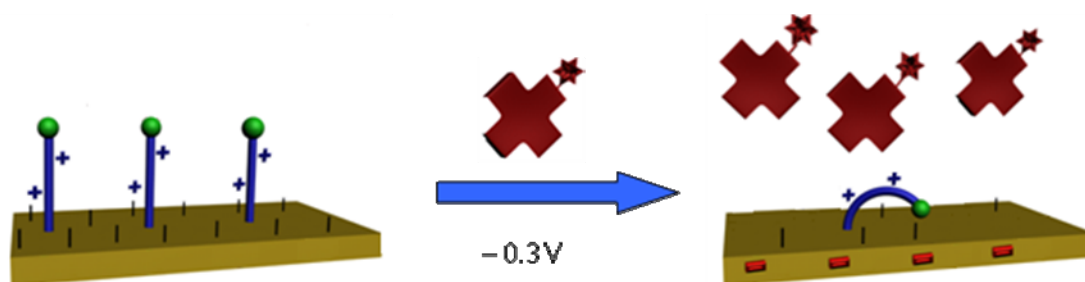
Figure 5.6. *Schematic of mixed SAMs showing a semi-desorbed monolayer due to the application of −0.3 V, thus less binding is observed in fluorescence images.*

5.3.1 Control Experiments

Control experiments were established with a similar sample of mixed SAMs consisting of TEGT and a peptide without biotin known as KKKKC. A ratio of 1:40 of KKKKC:TEGT was used to be consistent with the previous experiments and the XPS data. The control studies would also confirm the neutravidin binding was only occurring at the biotin binding sites.

The fluorescence images obtained (figure 5.7) indicate that there was almost no binding when both a positive and negative potential was applied to the surface. A complete zero intensity image was not observed as there will always be a small degree of non-specific binding, which occurs due to physisorption of neutravidin molecules on to the surface. The consistency of the fluorescent image intensities in figure 5.7 indicates that neutravidin binding is primarily occurring due to the biotin binding sites.
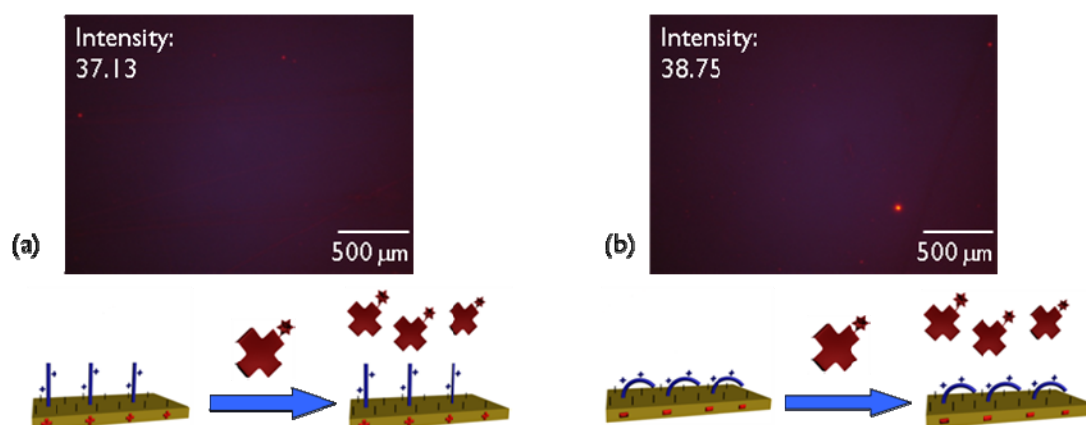
Figure 5.7. *Fluorescent images of a mixed SAMs surface with KKKKC and TEGT with an applied potential of (a) +0.3 V and (b) −0.3 V in the presence of fluorescently labelled neutravidin*

5.4   Cyclic Voltammetry Stability Studies

In order to understand the stability of the pure and mixed SAMs under an applied potential, cyclic voltammetry (CV) studies were carried out to find a suitable potential window of stability. To prevent oxygen and other contaminants affecting CV curves, the electrolyte was purged with Ar for 20 minutes prior to carrying out CV. Thereafter the electrochemical cell was sealed with a balloon filled with argon, thus ensuring experiments were carried out under an Ar environment. All CV experiments were carried out in a phosphate buffer solution at pH 7.4 following an overnight immersion of the polycrystalline gold electrode in a SAM solution.

5.4.1 Electrochemical Stability of Pure SAMs

Figure 5.8 presents the cyclic voltammograms obtained from the pure biotin-KKKKC and pure TEGT SAMs. Pure TEGT SAMs exhibit two cathodic peaks at -0.81 V and -1.01 V, which can be attributed to the reductive desorption of a thiol SAM from a polycrystalline gold surface.[70] Pure biotin-KKKKC SAMs shows the onset of reductive desorption occurring at around -0.5 V and a small cathodic peak appearing at -0.74 V.
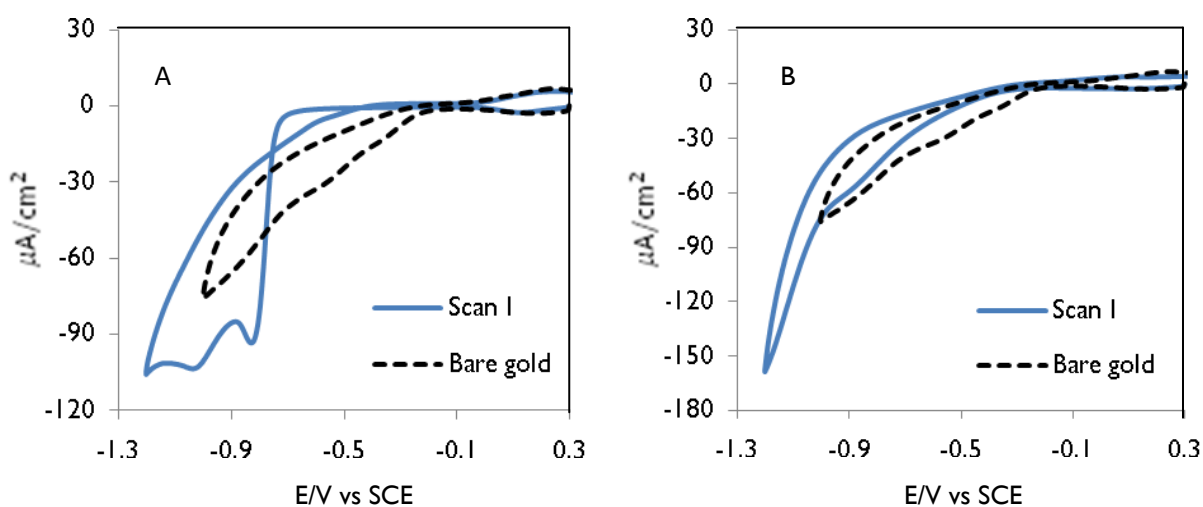
Figure 5.8. *Reductive desorption of (A) pure TEGT SAMs and (B) pure biotin-KKKKC SAMs on modified gold electrodes recorded in phosphate buffer solution, pH 7.4, at a 50 mV s^{-1}.*

5.4.2 Electrochemical Stability of Mixed SAMs

CV results for the mixed SAMs are presented in figure 5.9 where there is a cathodic peak initially at −0.88 V and a further cathodic peak appears at −1.05 V. This behaviour can be attributed to the reductive desorption of the SAMs, which is well known for SAMs of sulphur containing compounds on gold.[70]

After the first scan, it appears that the cleavage of the sulphur-gold bonds of the mixed SAM occurred progressively, with each scan removing more molecules. As molecules on the

surface begin to desorb into the bulk PBS solution, the peptide and TEGT surface concentration gradually decreases, thus the increase in current potential at ~ +0.3 V is due to phosphate anions in the electrolyte adsorbing onto the surface of the electrode.[42]
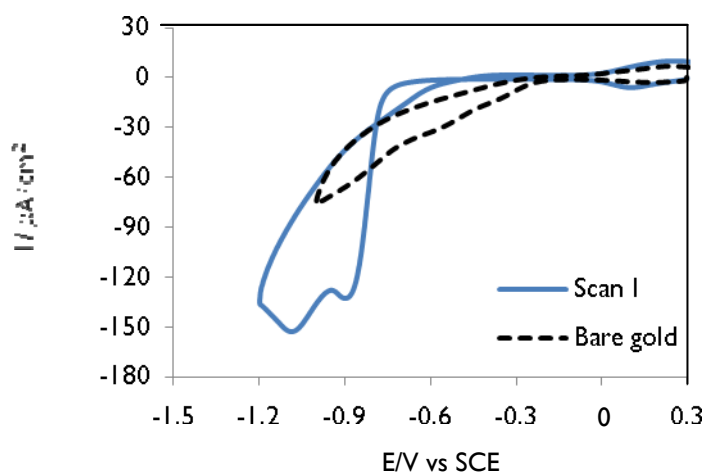
Figure 5.9. *Reductive desorption of mixed SAMs on modified gold electrodes recorded in phosphate buffer solution, pH 7.4, at a 50 mV s⁻¹.*

Reductive desorption of mixed SAMs in PBS solution on different samples of gold substrates showed multiple peaks. The varying desorption peaks observed for the pure TEGT and mixed SAMs desorption peaks are due to the presence of multiple crystal surfaces, each of which result in a slightly different energy of desorption.[70,81] The charge density of the mixed SAMs determined from an average of 3 samples was 1121.53 ± 74.6 $\mu A\ cm^{-2}$. The charge density determined was significantly greater than values found in previous work.[70] The primary cause of the large apparent charge density was due to the larger than expected desorption currents of ~150 $\mu A\ cm^{-2}$ (figure 5.9.). High currents obtained in these sets of experiments do not allow for surface coverage calculations due to unrealistic values.

In order to understand the high currents observed in the pure and mixed SAMs cyclic voltammograms, well-known SAMs were studied under the same system to identify the cause of the high currents.

5.4.3 Electrochemical Stability of Pure Octadecanethiol (ODT) SAMs

ODT SAMs have been previously characterised by CV with desorption occurring at -0.8 V.[82] The issue of high current densities observed at the region of reductive desorption was still present in the voltammogram shown in figure 5.10. The current of the ODT reductive desorption peak observed in figure 5.10 was almost 100 times larger with a PBS electrolyte compared to K_2SO_4 electrolyte used in literature.[82]
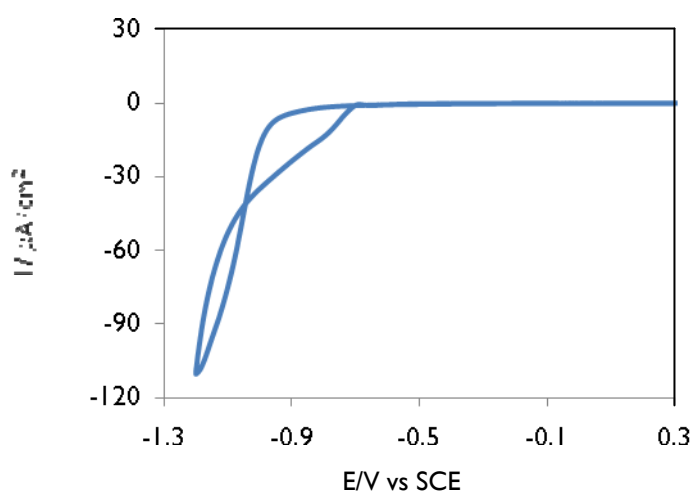

Figure 5.10. *Reductive desorption of ODT SAMs on modified gold electrodes recorded in phosphate buffer solution, pH 7.4, at a 50 mV s^{-1}.*

5.4.4 Electrochemical Stability Nitrophenolthiol (NPT) SAMs

CV was carried out on NPT SAMs in order to compare the NPT CV curve with literature and identify the cause of the large currents that have been observed throughout the CV studies. Conversion of the nitro group to an amine group is observed in the first scan, as has been reported in the literature.[47] The shape of the first scan (blue line) of the nitro group shows a double conversion peak instead of one peak, which is normally the case (figure 5.11). After the nitro conversion peak, hydrogen evolution appears along with a large increase in the current reaching almost 120 µA cm^{-2}.
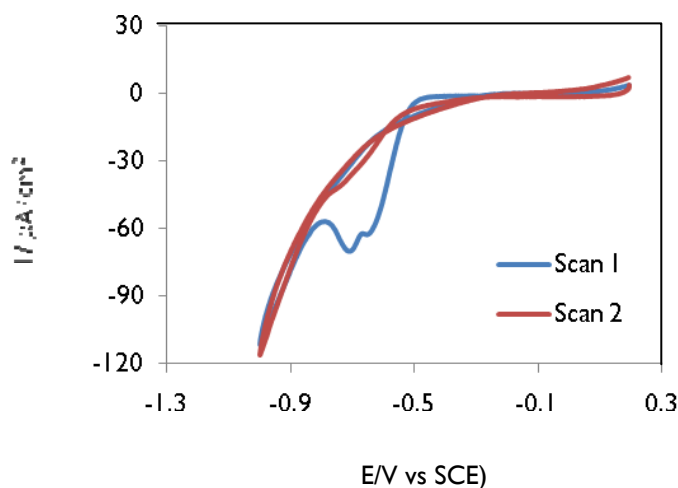
Figure 5.11. *Cyclic voltammogram of NPT SAMs on modified gold electrodes recorded in phosphate buffer solution, pH 7.4, at a 50 mV s^{-1}.*

6.5   Summary of CV Studies

The electrochemical stability of biotin-KKKKC and TEGT mixed SAMs on polycrystalline gold electrodes is difficult to quantify at this stage. The ability to integrate the reductive desorption peaks in order to be able to quantify the stability of the mixed SAMs has not been possible with a PBS electrolyte. Although PBS maybe an adequate electrolyte to use for the observation of reductive desorption,[42] PBS is not suitable for use in the stability studies of our mixed SAMs.

Oxygen content can play a significant role in the stability and desorption of SAMs,[68] hence all experiments were carried out under Ar-purged solutions, thus eliminating oxygen as a cause of high current. By investigating the reductive desorption of several different monolayers such as ODT, NPT, mixed SAMs, pure peptide and pure TEGT SAMs it has been possible to conclude that the use of PBS causes excessively high current densities, which does not allow for accurate estimations of surface coverage. The primary reason for the high current is due

to the fact that the hydrogen evolution peak overlaps with reductive desorption peaks when using PBS as an electrolyte[83] and a polycrystalline gold surface.[84]

There are a number of methods of reducing the effects of hydrogen evolution, which can be applied in any future stability studies. Two methods will be mentioned here:

1) Changing the electrolyte

   By altering the PBS solution to a more reliable electrolyte such as KOH[48,83] will help in shifting the hydrogen evolution peak away from the desorption peak. The KOH solution would shift the hydrogen evolution peak due to the much greater number OH^- ions and fewer H^+ ions in the solution. Other solutions such as NaOH,[83] LiOH[83] and KCl[83] have all been reported as suitable electrolytes for SAM stability studies using CV.

2) Altering gold surface

   In this project the gold used was polycrystalline gold, which has all three types of gold surfaces (111), (110) and (100). It has been reported in previous work[84] that a (111) gold surface can separate the reductive desorption peak and hydrogen evolution peak, by shifting the desorption peak to a less negative potential.

The objective stated in section 3 of understanding the stability of the mixed SAMs via an applied potential was not fully achieved due to the problems encountered regarding high currents and difficulties in measuring surface coverage. However, a better understanding of stability studies using CV has been gained overall and thus, future stability studies will be carried out accordingly.

6   Conclusion and Future Work

In this work it was shown via fluorescence microscopy that mixed monolayers with biotin-KKKKC and TEGT at a 1:40 solution ratio can be switched by applying a potential of − 0.3 V. Fluorescence images indicated that less binding took place between the neutravidin and the biotinylated peptide under a negative potential due to decreased image intensity. Control experiments were also carried out using non-biotinylated peptides to show that there was minimal non-specific binding and that binding only occurred on the biotin binding sites.

Stability studies were also carried out using cyclic voltammetry to check the stability range of the mixed monolayers, but due to high current densities, which resulted in unrealistic charge densities it was not possible to work out the exact surface coverage for a positively and negatively applied potential to a mixed monolayer. From the stability studies it was further understood that PBS as an electrolyte produces inaccurate measurements in charge density due to hydrogen evolution occurring in the region of the desorption peak. Furthermore by using polycrystalline gold, the hydrogen evolution peak could not be separated from the desorption peak.

In future, techniques such as surface plasmon resonance (SPR) would give a more accurate indication of protein binding due to its ability to quantify molecular binding on the surface. Stability studies are best carried out in KOH electrolyte with a (111) gold surface as these two factors can shift the hydrogen peak away from the desorption peak, thus giving the ability to accurately calculate charge density and surface coverage.

7   References

1. F. Schreiber, *Progress in Surface Science*, **2000**, *65*, 151

2. A. Ulman, *An Introduction to organic thin films from Langmuir-Blodgett to Self-Assembly*, **1991**, Academic Press

3. N. Tillman, A. Ulman, J. S. Schildkraut, T. L. Renner, *Journal of American Chemical Society*, **1988**, *110*, 6136

4. J. Lahann, S. Mitragotri, T. N. Tran, H. Kaido, J. Sundaram, I. S. Choi, S. Hoffer, G. A. Somorjai, R. Langer, *Science*, **2003**, *299*, 371

5. M. Mrksich, *Chemical Society Reviews,* **2000**, *29*, 267

6. F. Schreiber, *Journal of Physical Condensed Matter,* **2004**, *16*, R881

7. S. Onclin, B. J. Ravoo and D. N. Reinhoudt, *Angewandte Chemistry International Edition*, **2005**, *44*, 6282

8. G. A. Somerjai, *Chemistry in Two Dimensions – Surfaces*, **1982**, Cornell University Press: Ithaca, New York

9. M. W. Walczak, C. Chung, S. M. Stole, C. A. Widrig and M. D. Porter, *Journal of American Chemical Society,* **1991**, *113,* 2370

10. R. G. Nuzzo, B. R. Zegarski and L. H. Dubios, *Journal of American Chemical Society*, **1987**, *109, 733*

11. L. H. Dubois and R. G. Nuzzo, *Annual Review of Physical Chemistry.* **1992**, *43, 437 -*

12. C. D. Bain, E. B. Troughton, Y.–T. Tao, J. Evall, G. M. Whitesides, R. G. Nuzzo, *Journal of American Chemical Society*, **1989**, *111*, 321

13. A. N. Parikh, B. Liedberg, S. V. Atre, M. Ho, D. L. Allara, *Journal of Physical Chemistry*, **1995**, *99*, 9996

14. C. D. Bains, G. M. Whitesides, *Angewandte Chemistry International Edition*, **1989**, *28*, 506

15. L. T. Zhuravlev, *Langmuir*, **1987**, *3*, 316

16. C. K. Luscombe, H. –W. Li, T. S. Huck, A. B. Holmes, *Langmuir*, **2003**, *19*, 5273

17. P. Silberzan, L. Le´ger, D. Ausserre´, J. J. Benattar, *Langmuir*, **1991**, *7,* 1647

18. Wasserman, S. R.; Tao, Y. -T.; Whitesides, J. M. *Langmuir* **1989**, *5,* 1074

19. O. Dannenberger, M. Buck, M. Grunze, *Journal of Physical Chemistry B*, **1999**, *103*, 2202

20. C. D Bain, J. Evall, G. M Whitesides, *Journal of American Chemistry Society*, **1989**, *111*, 7164

21. K. E. Nelson, L. Gamble, L. S. Jung, M. S. Boeckl, E. Naeemi, S. L. Golledge, T. Sasaki, D. G. Castner, C. T. Campbell and P. S. Stayton, *Langmuir*, **2001**, *17*, 2807

22. H. C. Hays, P. A. Millner, M. I. Prodromidis, *Sensors and Actuators B*, **2006**, 1064

23. W. Senaratne, L. Adruzzi and C. K. Ober, *Biomacromolecules*, **2005**, *6*, 2427

24. K. L. Prime and G. M. Whitesides, *Journal of American Chemical Society*, **1993**, *115*, 10714

25. M. Zheng and X. Huang, *Journal of American Chemical Society*, **2004**, *126*, 12047

26. P.M. Mendes, *Chemical Society Reviews*, **2008**, *37*, 1

27. F. Zhou and W.T. S. Huck, *Physical Chemistry Chemical Physics*, **2006**, *8*, 3815

28. Y. Liu, L. Mu, B. H. Liu and J. L. Kong, *Chemistry - A European Journal*, **2005**, *11*, 2622

29. H. Nandivada, A. M. Ross, J. Lahann, *Progress in Polymer Science*, **2010,** *35*, 141

30. S. Ferretti, S. Paynter, D. A. Russell, K. E. Sapsford and D. J. Richardson, *Trends in Analytical Chemistry*,   **2000**, *19*, 530

31. N. Katsonis, M. Lubomska, M. M. Pollard, B. L. Feringa and P. Rudolf, *Progress in Surface Science*, **2007**, *82,* 407

32. C. J. Barrett, J. I. Mamiya, K. G. Yager and T. Ikeda, *Soft Matter*, **2007,** 3, 1249

33. P. B. Wan, Y. G. Jiang, Y. P. Wang, Z. Q. Wang and X. Zhang, *Chemical Communications*, **2008,** 5710

34. K. Ichimura, Y. Suzuki, T. Seki, A. Hosoki and K. Aoki, *Langmuir*, **1988**, *4*, 1214–6

35. Y. Liu, L. Mu, B. H. Liu, S. Zhang, P. Y. Yang, J. L. Kong, *Chemical Communications*, **2004**, *10*, 1194

36. L. Mu, Y. Liu, S. Y. Cai and J. L. Kong, *Chemical European Journal*, **2007**, *13*, 5113

37. B. Zhao, W. J. Brittain, W. S. Zhou and S. Z. D. Cheng, *Journal of American Chemical Society*, **2000**, *122*, 2407

38. M. Motornov, S. Minko, K. J. Eichhorn, M. Nitschke, F. Simon and M. Stamm, *Langmuir*, **2003**, *19*, 8077

39. Y. Liu, S. Meng, L. Mu, G. Jin, W. Zhong and J. Kong, *Biosensors and Bioelectronics*, **2008**, *24*, 710

40. S. Yasutomi, T. Morita and S. Kimura, *Journal of American Chemical Society*, **2005**, *127*, 14564

41. S. T. Wang, H. J. Liu, D. S. Liu, X. Y. Ma, X. H. Fang and L. Jiang, *Angewandte Chemie International Edition,* **2007**, *46*, 3915

42. T. Doneux, L. Bouffier, L. V. Mello, D. J. Rigden, I. Kejnovska, D. G. Fernig, S. J. Higgins, and R. J. Nichols, *Journal of Physical Chemistry C,* **2009,** *113,* 6792

43. W. Senaratne, L. Andruzzi and C. K. Ober, *Biomacromolecules*, **2005**, *6*, 2427

44. G. B. Sigal, C. Bamdad, A. Barberis, J. Strominger, G. M. Whitesides, *Analytical Chemistry*, **1996**, *68*, 490

45. S. Kossek, C. Padeste, L. X. Tiefenauer, H. Siegenthaler, *Biosensors and Bioelectrons*, **1998**, *13*, 31

46. E. W. L. Chan and M. N. Yousaf, *Journal of American Chemical Society*, **2006**, *128*, 15542

47. P. M. Mendes, K. L. Christman, P. Parthasarathy, E. Schopf, J. Ouyang, Y. Yang, J. A. Preece, H. D. Maynard, Y. Chen and J. F. Stoddart, *Bioconjugate Chemistry*, **2007**, *18*, 1919

48. W. S. Yeo and M. Mrksich, *Langmuir*, **2006**, *22*, 10816

49. I. Y. Wong, M. J. Footer and N. A. Melosh, *Soft Matter*, **2007**, *3*, 267

50. M. Curreli, C. Li, Y. H. Sun, B. Lei, M. A. Gundersen, M. E. Thompson and C. W. Zhou, *Journal of American Chemical Society*, **2005**, *127*, 6922

51. W. S. Yang, S. E. Baker, J. E. Butler, C. S. Lee, J. N. Russell, L. Shang, B. Sun and R. J. Hamers, *Chemistry of Materials*, **2005**, *17*, 938

52. F. A. Armstrong, *Current Opinion in Chemical Biology*, **2005**, *9*, 110

53. D. H. Murgida and P. Hildebrandt, *Physical Chemistry Chemical Physics*, **2005**, *7*, 3773

54. I. Willner and B. Willner, *Trends in Biotechnology*, **2001**, *19* 222

55. G. Gilardi and A. Fantuzzi, *Trends in Biotechnology*, **2001**, *19*, 468

56. C. S. Lee, S. E. Baker, M. S. Marcus, W. S. Yang, M. A. Eriksson and R. J. Hamers, *Nano Letters*, **2004**, *4*, 1713

57. D. Chow, M. L. Nunalee, D. W Lim, A. J. Simnick, A. Chilkoti, *Materials Science and Engineering R*, **2008**, *62*, 125

58. P. Ihalainen, J. Peltonen, *Sensors and Actuators B*, **2004**, *102*, 207

59. S. Hleli, C. Martelet, A. Abdelghani, N. Burais, N. Jaffrezic-Renault, *Sensor and Actuators B*, **2005**, *113*, 711

60. M. Mrksich, *Materials Research Society Bulletin*, **2005**, *30*, 180

61. D. P. Woodruff and T. A. Delchar, Modern Techniques of Surface Science - Second Edition, **1994**, *Cambridge University Press*

62. M. W. J. Beulen, M. I. Kastenberg, F. C. J. M. van Veggel and D. N. Reinhoudt, *Langmuir*, **1998**, *14*, 7463

63. D. K. Peng and J. Lahann, *Langmuir*, **2007**, *23*, 10184

64. R. Brito, R. Tremont and C. R. Cabrera, *Journal of Electronalytical Chemistry*, **2004**, *574*, 15

65. T-N. T. Tran, *PhD Thesis California Institute of Technology*, **2003**

66 A. Hamelin, M. J. Sottomayor, F. Silva, S.-C. Chang and M. J. Weaver, *Journal of Electroanalytical Chemistry*, **1990**, *295*, 291

67. W. R. Everett, T. L. Welch, L. Reed and I. Fritsch-Faules, *Analytical Chemistry*, **1995**, *67*, 292

68. W. R. Everett and I. Fritsch-Faules, *Analytica Chimica Actta*, **1995**, *307*, 253

69. D. E. Weisshaar, B. D. Lamp and M. D. Porter, *Journal of American Chemical Society*, **1992**, *114*, 5850

70. D.- F. Yang, C. P. Wilde and M. Morin, *Langmuir*, **1997**, *13*, 243

71. D. M. Lemay and J. L. Shepherd, *Electrochimica Acta*, **2008**, *54*, 388

72. http://www.microscopyu.com/articles/fluorescence/fluorescenceintro.html

73. J. R. Wayment and J. M. Harris, *Analytical Chemistry*, **2009**, *81*, 336

74. C. S. Tang, M. Dusseiller, S. Makohliso, M. Heuschkel, S. Sharma, B. Sharma, B. Keller and J. Vrs, *Analytical Chemistry*, **2006**, *78*, 711

75. S. X. Huang and Y. Chen, *Nano Lettters*, **2008**, *8*, 2829

76. L. Strong and G. M. Whitesides, *Langmuir*, **1988**, *4*, 546

77. P. E. Laibinis, M. A. Fox, J. P. Folkers and G. M. Whitesides, *Langmuir* **1991**, *7*, 3167

78 . H. Wang, S. Chen L. Li and S. Jiang, *Langmuir*, **2005**, *21*, 2633

79. M.Antonieta, D. Millone, H. Hamdoudi, L. Rodriguez, A. Rubet, G. A. Benitez, M. E. Vela, R. C. Salvarezza, J. E. Gayone, E. A. Sanchez, O. Grizzi, C. Dablemont and V. A. Esaulov, *Langmuir*, **2009**, *25*, 12945

80. C. D. Bain and G. M. Whitesides, *Angewandte Chemie International Edition*, **1989**, *28*, 506

81. W. R. Everett, I. Fritsch-Faules, *Analytica Chimica Acta*, **1994**, *307*, 253

82. J. A. N. Sondag-Huethorst and L. G. J. Fokkink, *Langmuir*, **1992**, *8*, 2560

83. G. Sanchez-Pomales, L. Santiago-Rodriguez, N. E. Rivera-Velez, C. R. Cabrera, *Journal of Electroanalytical Chemistry*, **2007**, *611*, 80

84. D. F. Yang, C. P. Wilde and M. Morin, *Langmuir*, **1996**, *12*, 6570